

UNCLASSIFIED

AD 275 102

*Reproduced
by the*

**ARMED SERVICES TECHNICAL INFORMATION AGENCY
ARLINGTON HALL STATION
ARLINGTON 12, VIRGINIA**



UNCLASSIFIED

NOTICE: When government or other drawings, specifications or other data are used for any purpose other than in connection with a definitely related government procurement operation, the U. S. Government thereby incurs no responsibility, nor any obligation whatsoever; and the fact that the Government may have formulated, furnished, or in any way supplied the said drawings, specifications, or other data is not to be regarded by implication or otherwise as in any manner licensing the holder or any other person or corporation, or conveying any rights or permission to manufacture, use or sell any patented invention that may in any way be related thereto.

275102

U. S. A R M Y
TRANSPORTATION RESEARCH COMMAND
FORT EUSTIS, VIRGINIA

275 102

TCREC TECHNICAL REPORT 61-142

**THEORETICAL INVESTIGATION OF THE FLUTTER
CHARACTERISTICS OF A JET-FLAP ROTOR SYSTEM
IN HOVERING FLIGHT**

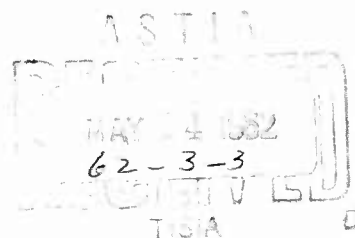
Task 9R38-13-014-03

Contract DA-44-177-TC-699

November 1961

prepared by:

CORNELL AERONAUTICAL LABORATORY, INC.
Buffalo, New York



FOREWORD


The work described in this report was accomplished by the Cornell Aeronautical Laboratory, Inc. (CAL), Buffalo, New York, for the U. S. Army Transportation Research Command (USATRECOM), Fort Eustis, Virginia. The work was accomplished under task 9R38-13-014-03, "Jet-Flap Rotor Investigations." Mr. Peter Crimi and Mr. Richard P. White of CAL conducted the study, and Mr. John E. Yeates administrated the project for USATRECOM. The work started 26 September 1960 and was completed 20 October 1961.

The report has been reviewed by the USATRECOM and is considered to be technically sound. The report is published for the exchange of information and the stimulation of ideas.

FOR THE COMMANDER:

APPROVED BY:


JOHN E. YEATES
USATRECOM Project Engineer


EARL A. WIRTH
CWO-4 USA
Adjutant

Task 9R38-13-014-03

Contract DA 44-177-TC-699

November 1961

THEORETICAL INVESTIGATION OF THE FLUTTER CHARACTERISTICS OF
A JET-FLAP ROTOR SYSTEM IN HOVERING FLIGHT

CAL REPORT BB-1493-S-1

Prepared by

Cornell Aeronautical Laboratory, Inc.
Buffalo, New York

for

U. S. Army Transportation Research Command
Fort Eustis, Virginia

ACKNOWLEDGMENTS

Appreciation is extended by the authors to Mr. Frank A. DuWaldt, of Cornell Aeronautical Laboratory, Inc., for the significant contributions he made to the investigation. The authors also wish to thank the U. S. Army Transportation Research Command and the Giravions-Dorand Company, Paris, France, for their cooperation in helping to establish the physical characteristics of a suitable jet-flap rotor system for use in the present investigation.

TABLE OF CONTENTS

	Page
FOREWORD.....	i
LIST OF ILLUSTRATIONS.....	vi
LIST OF SYMBOLS.....	vii
SUMMARY.....	1
CONCLUSIONS.....	2
RECOMMENDATIONS.....	4
I. INTRODUCTION.....	5
II. DESCRIPTION OF ROTOR SYSTEM ANALYZED.....	6
III. METHOD OF ANALYSES.....	8
IV. PRESENTATION AND DISCUSSION OF RESULTS.....	9
V. BIBLIOGRAPHY.....	31
APPENDIX I "DERIVATION OF FLUTTER DETERMINENT ELEMENTS".....	39
APPENDIX II "DERIVATION OF QUASI-STEADY AERO-DYNAMIC COEFFICIENTS FOR A TWO-DIMENSIONAL JET-FLAP AIRFOIL.....	54
DISTRIBUTION.....	57

LIST OF ILLUSTRATIONS

Figure		Page
1.	Planform Geometry of Blade Analyzed	17
2.	Nondimensional Mass and Vertical Bending Stiffness vs. Percent Radius	18
3.	Bending and Torsional Mode Deflections vs. Percent Radius	19
4.	Mode Frequency vs. Rotor Rotational Speed	20
5.	Schematic Representation of Two-Bladed Jet-Flap Rotor	21
6.	Comparison of γ and $\frac{\bar{\omega}_{\phi_1}}{\Omega}$ vs. $\frac{\bar{\omega}_{\theta_1}}{\bar{\omega}_{\phi_1}}$ for Different Elastic Axis Positions	22
7.	γ and $\frac{\bar{\omega}_{\phi_1}}{\Omega}$ vs. Jet Blowing Coefficient C_{J_0}	23
8.	γ and $\frac{\bar{\omega}_{\phi_1}}{\Omega}$ vs. Outboard CG Position	24
9.	Ω and ω vs. $\bar{\omega}_{\theta_1}$ Comparison of Effects of First and Second Bending Modes	25
10.	Comparison of γ and $\frac{\bar{\omega}_{\phi_1}}{\Omega}$ vs. $\frac{\bar{\omega}_{\theta_1}}{\bar{\omega}_{\phi_1}}$ with and without Teetering - $C_{J_0} = 0$	26
11.	Comparison of γ and $\frac{\bar{\omega}_{\phi_1}}{\Omega}$ vs. $\frac{\bar{\omega}_{\theta_1}}{\bar{\omega}_{\phi_1}}$ with and without Teetering - $C_{J_0} = 0.5$	27
12.	γ and $\frac{\bar{\omega}_{\phi_1}}{\Omega}$ vs. $\frac{\bar{\omega}_{\theta_1}}{\bar{\omega}_{\phi_1}}$ for Offset Rotor - CG at 25% Chord	28
13.	γ and $\frac{\bar{\omega}_{\phi_1}}{\Omega}$ vs. $\frac{\bar{\omega}_{\theta_1}}{\bar{\omega}_{\phi_1}}$ for Offset Rotor - CG at 35% Chord	29
14.	γ and $\frac{\bar{\omega}_{\phi_1}}{\Omega}$ vs. $\frac{\bar{\omega}_{\theta_1}}{\bar{\omega}_{\phi_1}}$ for Offset Rotor - No Teetering	30

LIST OF SYMBOLS

C_B	Blade Chord on Nontapered Section - ft.
C_F	Chord of Control Flap - ft.
C_{τ}	Blade Tip Chord - ft.
C_{T0}	Blowing Coefficient at Blade Tip - Nondimensional
$(CG)_0$	Center-of-gravity Position Over Outer 30% of Blade Radius- Percent of Chord
$(EA)_0$	Elastic Axis Position Over Outer 30% of Blade Radius- Percent of Chord
m	Mass Per Unit Length - Slugs/ft.
R	Blade Radius - ft.
β_1	Steady State Flapping Angle - Radians
$\Delta\beta_1$	Perturbation Flapping Angle - Radians
$\Delta\beta_2$	Perturbation Teetering Angle - Radians
δ_v	Vertical Offset of Blade Below the Teetering Axis - ft.
δ_h	Horizontal Offset of the Flapping Hinge from the Axis of Rotation- ft.
ν	Ratio of Flutter Frequency to Rotational Speed, $\frac{\omega}{\Omega}$ - Nondimensional
Ω	Rotational Speed - Cycles/sec.
ω	Flutter Frequency - Cycles/sec.
ω_{β_2}	Natural Frequency of the Teetering Mode - Cycles/sec.
$\bar{\omega}_{\theta_1}$	Nonrotating Torsional Frequency - Cycles/sec.
$\bar{\omega}_{\phi_1}$	Nonrotating First Bending Frequency - Cycles/sec.

LIST OF SYMBOLS - (Continued)

$\bar{\omega}_{\phi_2}$	Nonrotating Second Bending Frequency - Cycles/sec.
$\bar{\omega}_\tau$	Nonrotating Frequency of Jet-Flap Control - Cycles/sec.
$\Delta \phi_N$	Perturbation Bending Deflection at Blade Tip for N th Mode - ft.
$\Delta \theta_1$	Perturbation Torsional Deflection at Blade Tip for First Mode - Radians
$\Delta \tau$	Perturbation Rotation Angle of Jet-Flap with Respect to Blade Chord Line - Radians
θ_1	Steady State Torsional Deflection - Radians
τ	Steady State Rotation Angle of Jet-Flap with Respect to Blade Chord Line - Radians

SUMMARY

The purpose of the theoretical study reported herein was to investigate the aeroelastic characteristics of a jet-flap rotor system in hovering flight. The jet-flap rotor configuration assumed for this study incorporated most of the general characteristics of an experimental jet-flap rotor being developed for TRECOM by the Giravions-Dorand Company of Paris, France. On the basis of the investigation that was conducted, the following general conclusions were drawn regarding the dynamic and aeroelastic characteristics, over the normal range of operating conditions and parameter values, of a jet-flap rotor system in hovering flight.

1. The aeroelastic stability is insensitive to changes in the elastic-axis position or to changes in the nonrotating torsional-to-bending frequency ratio.
2. For a rotor having no teetering degree of freedom, the effects on the rotor stability of increased jet-blowing and aft movement of the center of gravity are similar and are destabilizing.
3. The dynamic characteristics of the jet-flap control may strongly influence the stability characteristics of a jet-flap rotor system.
4. Vertical offset of the flapping hinges of a doubly articulated rotor can have a very destabilizing influence. This effect, however, is not associated with the jet-flap characteristics of the rotor system.
5. Horizontal offset of the flapping hinges does not affect the stability characteristics of the rotor system.

CONCLUSIONS

On the basis of the results obtained, the following conclusions can be drawn regarding the general vibration and aeroelastic characteristics of jet-flap rotor systems in hovering flight.

1. A jet-flap rotor system, in which the jet provides both the control and propulsive forces, can be expected to have natural vibration frequencies appreciably higher than those associated with conventional rotors.
2. The effect of increasing the ratio of the nonrotating torsion frequency to the first bending frequency is stabilizing for low values of this ratio. For the range of frequency ratios expected to apply to practical jet-flap rotor systems $\omega_0/\omega_{\phi} > 5$, however, the aeroelastic stability characteristics of the rotor system are insensitive to frequency ratio.
3. For the assumed-jet-flap rotor system, the aeroelastic characteristics were insensitive to changes in the elastic axis location over the outer 30% of blade radius in the range of 15 to 25% chord.
4. For a rotor with no teetering degree-of-freedom, the effect of adding blowing to the rotor system is destabilizing, and the amount of destabilization is directly related to the amount of blowing.
5. With or without blowing, the rotor becomes more unstable in the symmetric modes as the chordwise center-of-gravity position is moved aft.
6. The effects of second bending should be included in any analyses that are conducted to determine, quantitatively, the aeroelastic characteristics of a specific jet-flap rotor system.
7. The dynamic characteristics of the control flap may strongly influence the aeroelastic stability of a jet-flap rotor configuration.
8. Vertical offset of the flapping hinges of a doubly articulated rotor can have a very destabilizing influence. This effect, however, is not associated with the jet-flap characteristics of the rotor system.

CONCLUSIONS (Continued)

9. Horizontal offset of the flapping hinges does not affect the stability characteristics of the rotor system.
10. Only symmetric types of instabilities will be encountered with a jet-flap rotor configuration having both teetering and flapping degrees of freedom if the vertical offset of the flapping hinge is zero.
11. If the vertical offset of the teetering hinge of a doubly articulated rotor is about 10% of the blade chord, only antisymmetric types of instabilities will be encountered.

RECOMMENDATIONS

On the basis of the results obtained and the analyses conducted, the following recommendations are made:

1. An unsteady aerodynamic theory for a jet-flap aerodynamic lifting surface should be developed.
2. A general investigation of the flutter characteristics of a jet-flap rotor system in forward flight should be conducted.
3. A thorough investigation of the effects of the jet-flap control system on the rotor stability characteristics should be conducted for a rotor system in both hovering and forward flight.
4. The detrimental aeroelastic effects caused by the vertical offset of the flapping hinge of a doubly articulated rotor should be thoroughly investigated for a nonblowing rotor system.

I. INTRODUCTION

Considerable effort has been applied to the theoretical and experimental study of the flutter of conventional helicopter rotors in hovering flight, (e.g., Refs. 1 through 8). These investigations have contributed to the understanding of the blade instabilities that have been encountered and have indicated means for avoiding such difficulties.

Recently there has been much interest in the development of a helicopter rotor system that applies the jet-flap principle to obtain both cyclic and collective pitch control as well as propulsion, (Refs. 9 and 10). Interest in the development of a jet-flap rotor derives from the gains in performance that may be obtainable through circulation and boundary layer control. A jet-flap rotor system should delay the adverse effects of blade stall and compressibility losses and increase the rotor thrust coefficient. In addition, this type of rotor should make obtainable the many advantages of torque transmission that are inherent in all tip-drive systems.

While flutter of conventional helicopter blades is the same phenomenon as wing flutter, certain effects of importance with respect to rotor blades are of little importance or nonexistent in fixed wings. These include gyroscopic or Coriolis couplings and elastic or inertial couplings introduced by hub mechanisms or control systems. In addition, the fact that a blade can pass through or close to vortices shed in previous revolutions makes it necessary to alter the conventional oscillating aerodynamic forces used in wing flutter analyses (Ref. 11). In spite of these additional complexities, there are theoretical methods, which, for practical engineering purposes, are adequate for estimating the flutter characteristics of a conventional rotor blade in hovering flight. Introduction of the jet-flap on a rotor, however, further increases the complexity of the flutter problem in that the aerodynamic forces arising from the jet reaction and super circulation must be included. These additional aerodynamics are such that their dynamic interactions with the mass and elastic forces may be different from those associated with the aerodynamic forces of a conventional rotor.

The results that are presented and discussed in this report were obtained by means of theoretical analyses that incorporate quasi-steady aerodynamics based on available jet-flap aerodynamic theories. For this reason and since a "representative" jet-flap rotor system was assumed, the work reported herein should be regarded primarily as an exploratory study to define potential aeroelastic problem areas associated with a jet-flap rotor system and to indicate means for circumventing dangerous flutter conditions.

II. DESCRIPTION OF ROTOR SYSTEM ANALYZED

1. GENERAL CHARACTERISTICS OF THE ROTOR

The jet-flap rotor system considered in the investigations reported herein was a two-blade symmetrical rotor having a teetering hinge on the axis of rotation and flapping hinges beneath the teetering hinge which were symmetrically offset from the axis of rotation. The cyclic and collective pitch control as well as the rotor torque was assumed to be supplied by the jet-flap located over the outer portion of the blade span. The requirements for a blade-pitch mechanism and a lead-lag hinge at the blade root are thus eliminated. It was assumed that the characteristics of the blowing over the outer portion of the blade radius was such that the jet momentum was constant along the span.

2. GEOMETRIC CHARACTERISTICS OF THE ROTOR SYSTEM

Figure 1 presents a sketch of the assumed rotor system. The blade planform has a constant chord from 20%R to 70%R and is then tapered in a linear manner to a tip chord of 67.5% of the main blade chord. The jet-flap is located at the trailing edge over the tapered outer 30% of the blade radius. It was assumed in the present study that when the jet flap rotates with respect to the blade chord a conventional flap also rotates through the same angle. The conventional flap was assumed to have a constant chord equal to $12\frac{1}{2}\%$ of the blade tip chord and to extend from the 70% radius station to the blade tip.

The horizontal offset of the flapping hinge, δ_h , was varied from zero to 5% of the blade radius, and the vertical offset of blade below the teetering hinge, δ_v , was varied from zero to 10% of the blade chord.

3. MASS AND ELASTIC CHARACTERISTICS OF THE ROTOR BLADES

Figure 2 presents the spanwise distribution of the mass and flapwise stiffness characteristics of the assumed jet-flap blade set. It is noted that the increase in both the mass and the flapwise bending stiffness near the root is not nearly as large as with conventional helicopter blades. With a conventional helicopter blade the flapwise bending stiffness at the blade root is on the order of 8 times that of the rest of the blade, and the mass per unit length near the blade root is on the order of at least 10 times that of the rest of the blade. As can be seen from Figure 2 for the assumed jet-flap blade configuration, the buildup of the flapwise bending stiffness and mass per unit length near the blade root is only on the order of 2 to 1. These differences

II. DESCRIPTION OF ROTOR SYSTEM ANALYZED (Continued)

are justified because the jet-flap rotor system obtains both its control and propulsion from the aerodynamic jet located near the tip of the blade. Therefore, the complex and heavier blade construction required to incorporate the lead-lag hinge and pitch control mechanism is avoided. This feature of the jet-flap rotor system results in a more rigid rotating blade set than is obtainable with conventional rotors.

The chordwise location of the blade elastic axis was assumed to be at the 25% chord over the nontapered blade sections (20% to 70%R). The elastic axis position over the blowing portion of the blade (70% radius to blade tip) was made a parameter in the calculations, because the structural characteristics of the open airfoil section over this portion of the blade are uncertain. Analyses were conducted for elastic axis positions at both the 15% and 25% chord over the blowing section of the blade. This range is believed to cover the limits of possible chordwise locations.

The center-of-gravity position was assumed to be at the 25% chord position over the nontapered blade sections (20% to 70% radius). Analyses were conducted for a range of center-of-gravity positions from 25% to 45% of the chord over the outboard portion of the blade (70% radius to blade tip).

4. VIBRATION CHARACTERISTICS OF THE ROTOR SYSTEM

On the basis of preliminary mass-elastic data estimated for an experimental jet-flap rotor system under development, a set of nonrotating and rotating flapwise bending and torsional mode shapes and frequencies were calculated by the method presented in Ref. 12. These mode shapes were used as the deformation modes in the flutter analyses reported herein. The nondimensional first three nonrotating bending mode shapes and first nonrotating torsional mode shape are presented in Fig. 3. Figure 4 presents a plot which shows the variation of the various mode frequencies with rotational speed.

As might be expected, the bending and torsional mode shapes presented in Fig. 3 for the jet-flap rotor are very similar to those of a conventional rotor. The bending and torsional mode frequencies and their variation with rotational speed are, however, quite different from those of a conventional helicopter blade. It is noted that the nonrotating frequencies of both the bending and torsional modes are much higher than those of the conventional helicopter blade, and, therefore, the variation of the various bending and torsional mode frequencies with rotational speed is not as pronounced. The primary reason for these different vibratory characteristics is due to the structural efficiency of the assumed jet-flap rotor blade.

III. METHOD OF ANALYSIS

1. EQUATIONS OF MOTION

The general equations of motion for helicopter rotor configurations, as derived by a Lagrangian approach, were developed and reported in Ref. 13. These general equations of motion were then used to develop specific equations of motion for the jet-flap rotor having flapping, teetering, bending, torsion and control flap degrees of freedom. Fig. 5 presents a schematic representation of the rotor system on which are noted the coordinate system, which rotates with the rotor system, and the generalized coordinates for the various degrees of freedom.

APPENDIX I presents the major steps in the development of the equations of motion as well as the expressions for the coefficients involved in these equations.

2. DERIVATION OF THEORETICAL EXPRESSIONS FOR THE AERODYNAMIC FORCES AND MOMENTS

At present there is no theory available which predicts the aerodynamic forces and moments on a jet-flap airfoil in unsteady motion with an accuracy approaching that of the theories developed for conventional airfoils. Past experience with the analysis of the aeroelastic characteristics of conventional rotor systems, (e.g., Ref. 13), indicates, however, that the use of steady aerodynamic theories in a quasi-steady approach to the oscillatory problem will at least indicate the major areas of instability.

For the analyses reported herein, the quasi-steady aerodynamic forces and moments were derived for the jet-flap airfoil using the steady aerodynamic theory developed by Hough in Ref. 14. In this reference Hough derived the lift and moment coefficients for a zero-thickness, two-dimensional, jet-flap airfoil with parabolic camber. An approximation for the lift and moment due to pitching velocity can be obtained from Hough's results since, under the quasi-steady assumption, a pitching rate is equivalent to a camber. For the aerodynamic forces arising from the oscillating jet-flap control, the approximate expressions developed by D. A. Spence in Ref. 15 were utilized. The derivation of the quasi-steady aerodynamic coefficients is presented in detail in APPENDIX II.

IV. PRESENTATION AND DISCUSSION OF RESULTS

In general, the theoretical results obtained were analyzed with the objective of determining the effects of various system parameters on the aeroelastic stability of a jet-flap rotor system. It should be emphasized that, since only a "representative" rotor system was analyzed, the results cannot be considered as a quantitative measure of the flutter characteristics of a jet-flap rotor system. The results do provide, however, an indication of the qualitative effects of system parameters. In the following sections, the effects of the torsion-to-bending frequency ratio, elastic axis position, center-of-gravity position, and blowing coefficient are discussed for each of two basic rotor systems.

The only difference between the rotor systems analyzed was the horizontal and vertical offset of the flapping hinge with respect to the axis of rotation and teetering hinge, respectively. One rotor system had zero horizontal and vertical offset of the flapping hinge. The flapping hinge of the second rotor system analyzed had a vertical offset of 10% of the blade chord and a horizontal offset of 5% of the blade radius.

A. ROTOR FOR WHICH THERE IS NO VERTICAL OR HORIZONTAL OFFSET OF THE FLAPPING HINGE

Figure 6 presents the variation of γ and $\frac{\bar{\omega}_{\phi_1}}{\Omega}$ with $\frac{\bar{\omega}_{\theta_1}}{\bar{\omega}_{\phi_1}}$ for two different outboard elastic axis stations. These plots were obtained for the blowing section of the blade having a CG position at the 35% chord, a blowing coefficient $C_{J_0} = 0.50$, and for the blade having 1st bending, 1st torsion, flapping and teetering degrees of freedom. It should be noted that the solutions to the theoretical equations of motion were obtained by assuming the flutter frequency ratio γ and then determining the value of $\bar{\omega}_{\phi_1}/\Omega$ and $\bar{\omega}_{\theta_1}/\Omega$ that satisfied the

flutter determinant. The graphs presented in Fig. 6, therefore, show the basic manner in which the results of the computer program were plotted. The crosshatched areas are the unstable regions and for given bending and torsional frequencies the unstable regions are approached from above as the rotational speed is increased. The characteristics of the curves presented in Fig. 6 are typical of those obtained for all the cases studied except for a forward CG location and no blowing.

The first mode of instability that is encountered as the rotational speed is increased is primarily a bending-torsion flutter mode. If this flutter mode could be traversed, an instability involving primarily the bending, torsion and flapping modes would be encountered. This

IV. PRESENTATION AND DISCUSSION OF RESULTS (Continued)

second boundary of neutral stability in an already unstable region is obtained because of the manner in which the equations of motion are solved. Since, however, the first instability cannot be traversed with increasing rotational speed, this second area of instability has little physical significance.

1. EFFECTS OF THE FREQUENCY RATIO

As can be seen from Fig. 6, the effect of increasing the frequency ratio $\bar{\omega}_\theta / \bar{\omega}_\phi$ is stabilizing. This result is not surprising, since

it reflects an increasing frequency separation of the bending and torsion modes. As might be expected, the most rapid changes in the stability occur near a frequency ratio of unity. For conventional rotors and for the assumed jet-flap rotor, the value of the frequency ratio is five or greater, and for these values the stability boundary is becoming very insensitive to frequency ratio. From the results presented in Fig. 6 it is thus concluded that the frequency ratio $\bar{\omega}_\theta / \bar{\omega}_\phi$, if above five, will not be a primary flutter parameter of jet-flap rotor systems.

2. EFFECTS OF ELASTIC AXIS POSITION

From the results plotted in Fig. 6, the effect of moving the elastic axis over the outboard spanwise sections can be determined. The results indicate that for the change in elastic axis position that was assumed, there is no appreciable effect on the flutter boundaries. The portion of the rotor blade over which the elastic axis was varied corresponds to the sections where the jet-flap is located. Over this section of the blade, the main structural member is an open section because of the nozzle and it is believed, therefore, that the elastic axis could be located between the 15 and 25% chord. On the basis of the results presented in Fig. 6, it might be concluded that if the elastic axis is located somewhere between the 15 and 25% chord over the outer 30% of the rotor span, its exact location is of little significance as regards flutter.

3. EFFECTS OF JET-BLOWING COEFFICIENT

Figure 7 presents the variation of the flutter frequency and rotor speed with increasing jet-blowing for a rotor having bending, torsion, flapping and teetering degrees of freedom. This figure was constructed

IV. PRESENTATION AND DISCUSSION OF RESULTS (Continued)

by crossplotting, at a given frequency ratio, results that were obtained for various blowing coefficients. The results indicate that for zero blowing coefficient, there is a single mode of instability; but for blowing coefficients greater than 0.05, there are two unstable modes. Again, a neutral stability boundary is theoretically obtainable in an already unstable region because of the technique that was used to solve the equations of motion. The effects of increased blowing on both flutter modes is destabilizing. The first flutter instability to be encountered with increasing RPM involves, primarily, the torsion mode with small amounts of bending and flapping and a trace of teetering motions. The frequency of this mode of instability is about 90% of the nonrotating torsional frequency for small C_{Jo} 's and increases with increasing C_{Jo} until it reaches approximately 95% of the nonrotating torsional frequency at $C_{Jo} = 2.0$. The flutter instability that exists at $C_{Jo} = 0$ is a more strongly coupled instability that involves all four degrees of freedom to an appreciable extent.

As is clearly indicated by the results plotted in Fig. 7, the destabilizing effect in the mode involving primarily the torsional degree of freedom is much more pronounced than that which involves stronger coupling among all modes. The exact reason for the different degrees of destabilization has not been determined, but it seems that the jet-flap has a destabilizing influence in the torsional degree of freedom and that when the bending and flapping modes are more strongly coupled with the torsional mode, this destabilizing influence is reduced. It should be noted that the destabilizing effect of jet blowing was not limited to the configuration for which the results are presented in Fig. 7 but was found for all the combinations of parameters investigated with both the three and four degree-of-freedom rotor systems (i.e., with and without teetering).

4. THE EFFECT OF THE CENTER-OF-GRAVITY POSITION

The results presented in Fig. 8 show the effects caused by a change in the center-of-gravity position over the outer 30% of blade span. These results show what might be expected; aft center-of-gravity positions are more unstable than center-of-gravity positions approaching the center of pressure. It should be noted that as the blowing coefficient is increased, the curves shown move to the left and up. Thus, with a given nonrotating bending frequency, additional blowing permits flutter to be obtained at a lower rotational speed and at a more forward position of the center of gravity.

IV. PRESENTATION AND DISCUSSION OF RESULTS (Continued)

5. EFFECT OF HIGHER BENDING MODES

Because many of the instabilities involving bending had flutter frequencies near the second bending mode frequencies, it was decided to investigate the importance of the second bending mode. Figure 9 compares the flutter characteristics of a rotor system having torsion, flapping, teetering, and either first or second bending as degrees of freedom. It should be noted that the instability occurring at the lower rotational speed has the higher flutter frequency (curve A). From the comparison of the results, it is noted that the critical instability determined on the basis of the second bending mode occurs at a higher rotational speed and at a lower frequency than the critical instability based on the first bending mode. On the basis of these results, it is concluded that the second bending mode might have an effect on the aeroelastic characteristics of the rotor system. Therefore, both bending modes should probably be included in any attempt to determine, on a quantitative basis, the flutter characteristics of a jet-flap rotor system. It is believed, however, that the neglect of the second bending mode did not appreciably affect the results that were obtained during the present program.

6. EFFECTS DUE TO THE DYNAMIC CHARACTERISTICS OF THE CONTROL FLAP

The preliminary results obtained, while not conclusive, indicate that the control flap may seriously affect the aeroelastic stability of the system and should therefore be studied in detail.

7. THE EFFECTS OF THE TEETERING DEGREE OF FREEDOM

Except for those configurations for which results are presented in Figs. 10 and 11, the presence of the hub teetering degree of freedom was found to have no effect on the flutter characteristics of the jet-flap rotor system having zero vertical and horizontal offset of the flapping hinge. It was noted that moving the center of gravity aft from the 25% chord or increasing the blowing coefficient suppressed the teetering flutter mode.

It can be seen from the results plotted in Fig. 10 for the nonblowing rotor configuration that the flutter characteristics having bending, torsion and flapping degrees of freedom are altered when the teetering degree of freedom is added. With the teetering degree of freedom present, only a torsion-teetering mode instability is obtained at approximately

IV. PRESENTATION AND DISCUSSION OF RESULTS (Continued)

the natural frequency of the teetering degree of freedom $\omega_{\beta_2} = 1.22 \Omega$ and is present only at very low torsion-to-bending frequency ratios. With the teetering degree of freedom removed, a bending-torsion-flapping mode instability is obtained for all torsion-to-bending frequency ratios above 0.25.

A comparison of the flutter characteristics of the rotor system with and without the teetering degree-of-freedom present is shown in Fig. 11 for a rotor with a blowing coefficient of 0.50. With teetering present, two flutter modes are obtained above a torsion-to-bending frequency ratio of 0.50.

The flutter boundary labeled "A" is primarily a bending-torsion-flapping mode instability and the loop labeled "B" is basically a torsion-teetering instability which occurs at the natural frequency of the teetering mode. With the teetering not present, only one flutter mode is obtained; and, as shown, its characteristics are almost identical to those of the bending-torsion-flapping instability associated with the rotor configuration that included the teetering degree of freedom.

Flutter modes that involve the teetering degree of freedom are basically antisymmetric modes of instability, and those that do not involve the teetering degree of freedom are symmetric. Except for the two configurations presented in Figs. 10 and 11, the addition of the teetering degree of freedom to a rotor system having bending, torsion, and flapping degrees of freedom did not alter the flutter characteristics of the rotor system. It might be concluded, therefore, that due to the aerodynamic couplings associated with a jet-flap rotor system, instabilities associated with antisymmetric degrees of freedom cannot be obtained. For example, with the configuration for which only an antisymmetric flutter instability was encountered (Fig. 10), the addition of jet blowing altered the flutter characteristics of the system so that only a symmetric type of instability was obtained.

The mass coupling between the teetering-flapping and teetering-bending mode is a direct function of the vertical offset of the flapping hinge. Since, for the configuration under consideration, this offset is very close to zero, the antisymmetric modes of the rotor system are very weakly coupled. It is not surprising, therefore, that the additional coupling between the various degrees of freedom caused by the addition of jet blowing results in the suppression of the antisymmetric flutter modes.

IV. PRESENTATION AND DISCUSSION OF RESULTS (Continued)

B. ROTOR FOR WHICH THERE IS A SIGNIFICANT HORIZONTAL AND VERTICAL OFFSET OF THE FLAPPING HINGES

Figure 12 presents the results obtained with the offset rotor having a blade chordwise center-of-gravity position corresponding to a balanced rotor blade and an intermediate value of the blowing coefficient. The blade configuration for which these results were obtained is the same as that used to obtain the results presented in Fig. 11 for a rotor having negligible offset of the flapping hinges. As in Fig. 11, the curve labeled "A" is an instability involving the symmetric degrees of freedom, and the curves labeled "B" are instabilities involving the antisymmetric degrees of freedom in which the teetering mode predominates. In comparing the results presented in Fig's. 11 and 12 it can be seen that the symmetric instabilities were not affected by the change in the offset of the flapping hinges but that the instabilities involving the antisymmetric degrees of freedom were altered radically. It is noted that the increase in the vertical offset of the flapping hinges changed the critical flutter mode from a symmetric to an antisymmetric instability and that in the frequency ratio range $1 \leq \bar{\omega}_\theta / \bar{\omega}_\phi \leq 6$, the rotor speed at which the critical instability occurs is independent of the frequency ratio. The critical antisymmetric instability is characterized by extremely large motions in the teetering degree of freedom and large motions in the bending and flapping degrees of freedom. While motions in the torsional degree of freedom are present, they are small compared to the motions in the other degrees of freedom.

The frequency at which the critical instability occurs is also constant and is equal to 70% of the bending frequency. This frequency is approximately equal to the natural frequency of one of the coupled bending-flapping-teetering modes of the rotor system. It is believed that the reason that the flutter frequency does not change with $\bar{\omega}_\theta / \bar{\omega}_\phi$ is that the torsional degree of freedom makes no appreciable contribution to this instability.

Except for the frequency ratio range near unity, flutter occurred at the same values of \mathcal{P} and $\bar{\omega}_\theta / \Omega$ over the range of blowing coefficient investigated, $0 \leq C_{j_0} \leq 2.0$. This result indicates that the instability is not necessarily associated with a jet-flap rotor configuration and can, in fact, be obtained with a non-blowing rotor that is doubly articulated. For this reason this mode of instability should be investigated further for a non-blowing doubly articulated rotor using

IV. PRESENTATION AND DISCUSSION OF RESULTS (Continued)

unsteady aerodynamics theories such as that developed by Loewy in Ref. 13.

Figure 13 presents the results obtained with the offset rotor having a blade chordwise center-of-gravity position corresponding to an unbalanced rotor blade and an intermediate value of the blowing coefficient. The heavier boundary corresponds to the instability associated with the antisymmetric degrees of freedom, and the lighter boundaries are the instabilities associated with the symmetric degrees of freedom. The requests presented are similar to those presented in Fig. 12 in that the critical flutter mode is associated with the antisymmetric degrees of freedom. The flutter frequency and critical rotational speed are identical with those for the more forward chordwise C.G. location and are independent of $\bar{\omega}_e / \bar{\omega}_\phi$, when this ratio is greater than 1.5. The unstable mode again has extremely large motions in the teetering degree of freedom and large motion in the bending and flapping degrees of freedom. The torsional degree of freedom is present in the instability, but the torsional amplitudes are small when compared with those in the other degrees of freedom.

As with the results presented in Fig. 12, the frequency and rotational speed of the critical flutter mode are found to be independent of the jet-blowing coefficient. From comparison of the results shown in Fig's. 12 and 13, it can be seen that the characteristics of the critical flutter mode do not change with the chordwise center-of-gravity position. Since the torsional degree of freedom was not predominant in this instability, and chordwise movement of the center of gravity only affects the coupling among the plunging and torsional degrees of freedom, this result is what might be expected.

Figure 14 presents results obtained for a jet-flap rotor having only a horizontal offset of the flapping hinge and no teetering degree of freedom. The results shown in this figure are identical with the results obtained for the rotor having no vertical or horizontal offset of the flapping hinge. Further, horizontal hinge offset was found to have no effect on the results over the whole range of blowing coefficients investigated. It may be concluded, therefore, that the horizontal offset of the flapping hinge relative to the rotation axis does not affect the symmetric flutter modes of the rotor system.

Comparison of the results presented in Fig. 14 with those presented in Fig. 13 for the symmetric flutter modes indicates that the symmetric modes are not appreciably affected by the vertical offset of the teetering

IV. PRESENTATION AND DISCUSSION OF RESULTS (Continued)

hinge, particularly at higher values of the frequency ratio.

On the basis of the results presented in Fig's. 12, 13 and 14 and the comparison of these results with those obtained with a rotor having no horizontal or vertical offset of the flapping hinges, it is concluded that increasing the vertical offset of the flapping hinges with respect to the teetering hinge can seriously compromise the aeroelastic stability of the rotor system. It is noted, too, that this instability is probably not just a characteristic of a jet-flap rotor system but might be obtained with any rotor system that has doubly articulated blades.

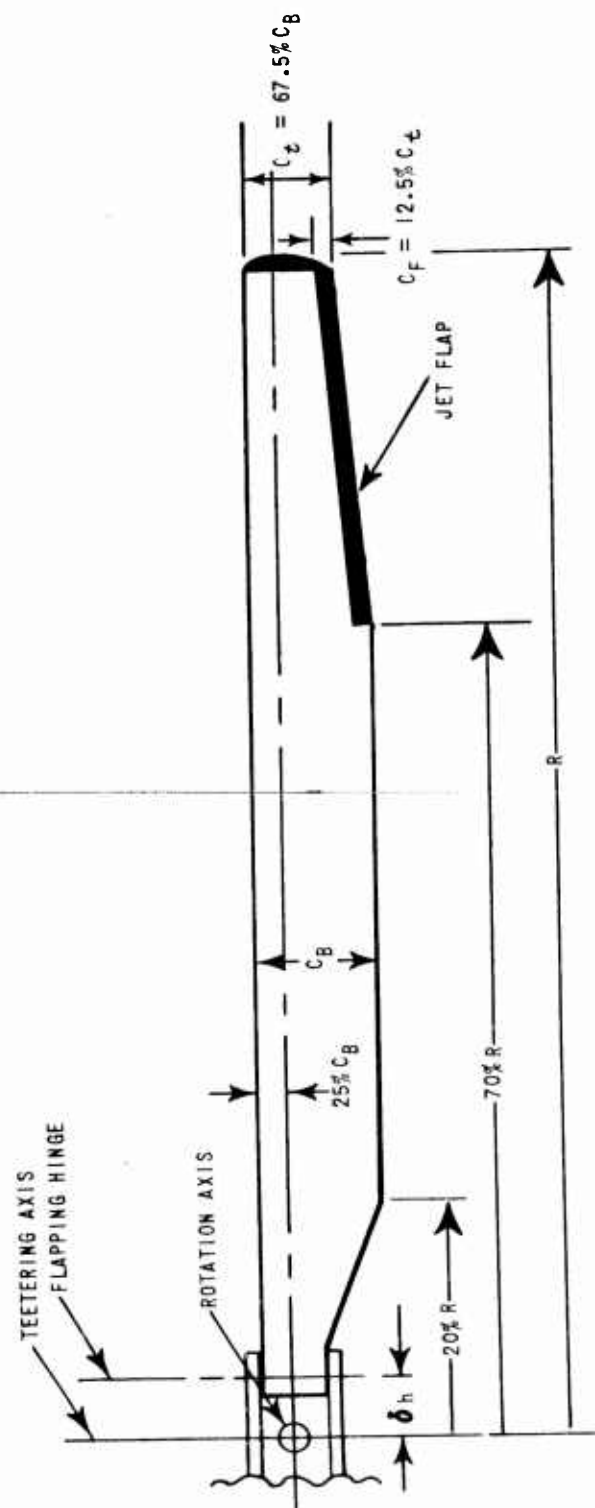


Figure 1. PLANFORM GEOMETRY OF BLADE ANALYZED

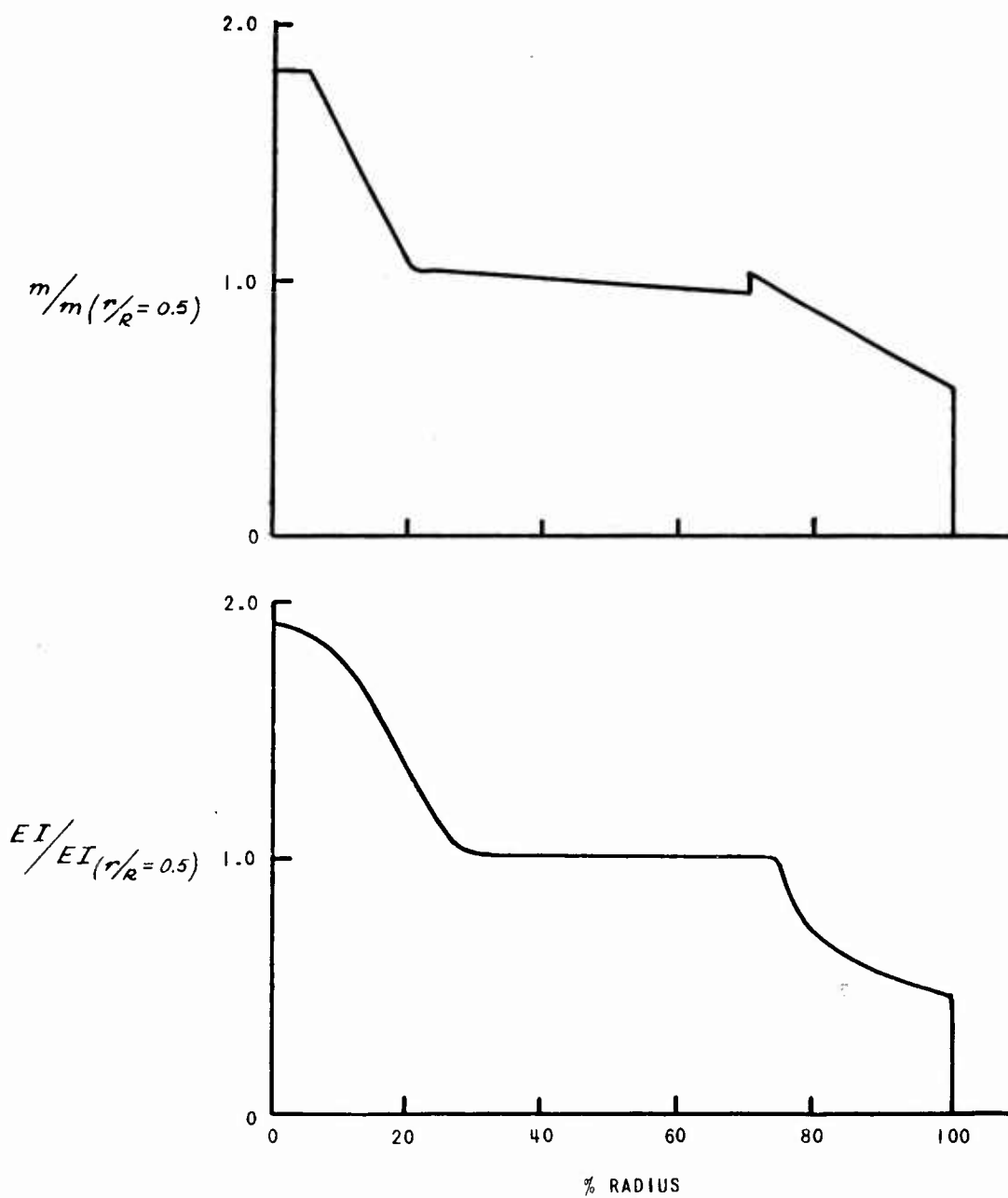


Figure 2. NONDIMENSIONAL MASS AND VERTICAL BENDING STIFFNESS
vs PERCENT RADIUS

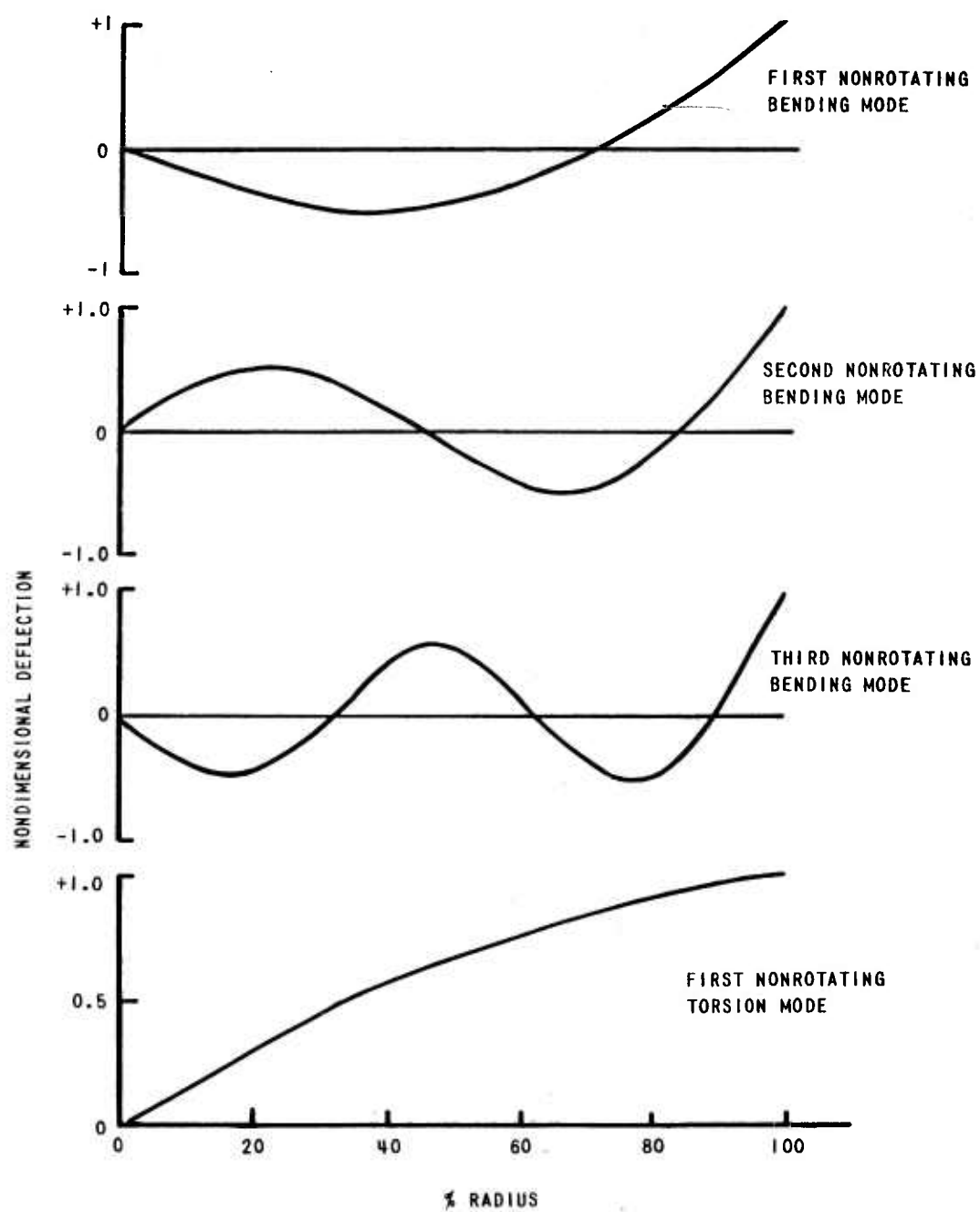


Figure 3. BENDING AND TORSIONAL MODE DEFLECTIONS vs PERCENT RADIUS

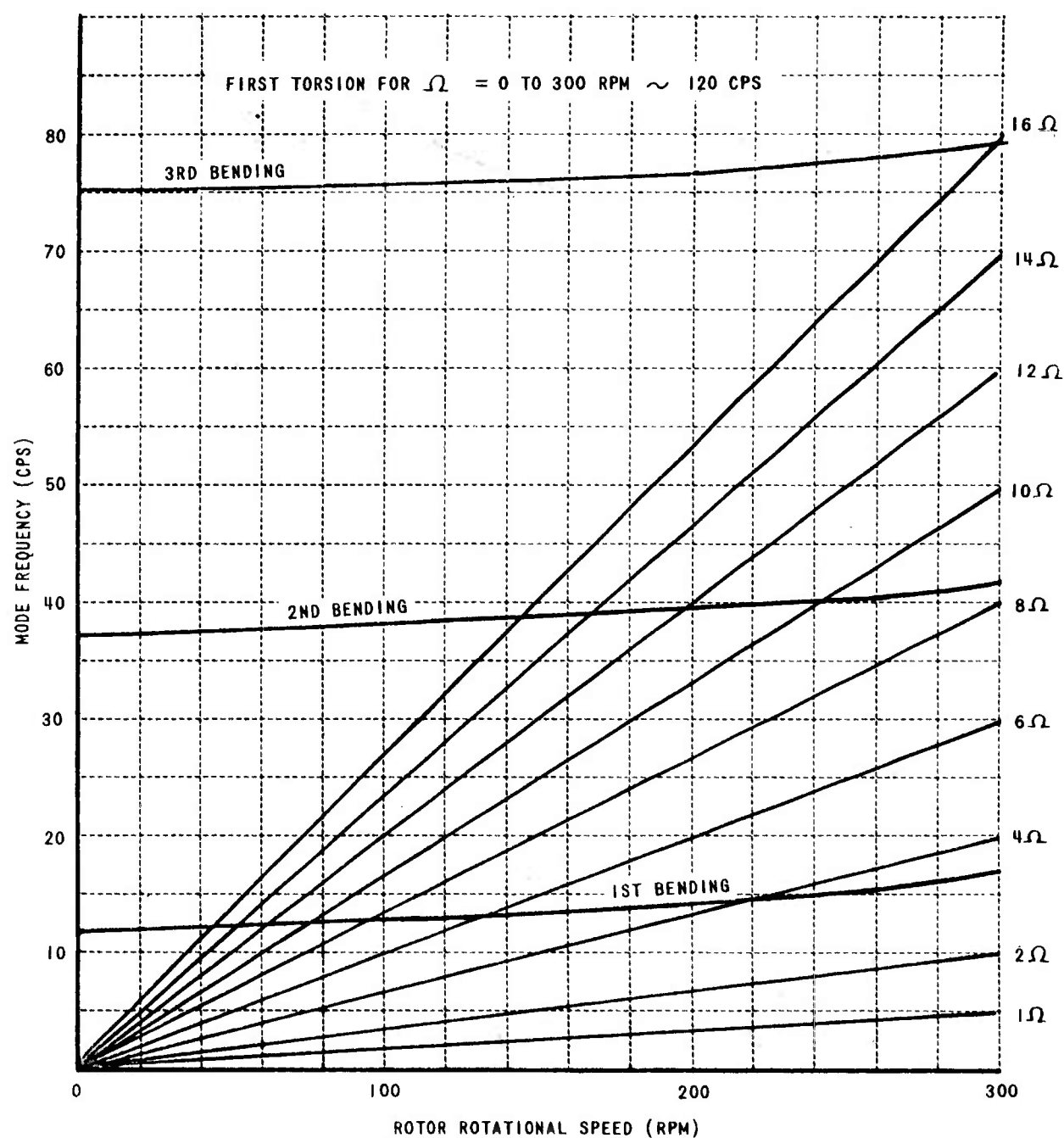


Figure 4. MODE FREQUENCY vs ROTOR ROTATIONAL SPEED

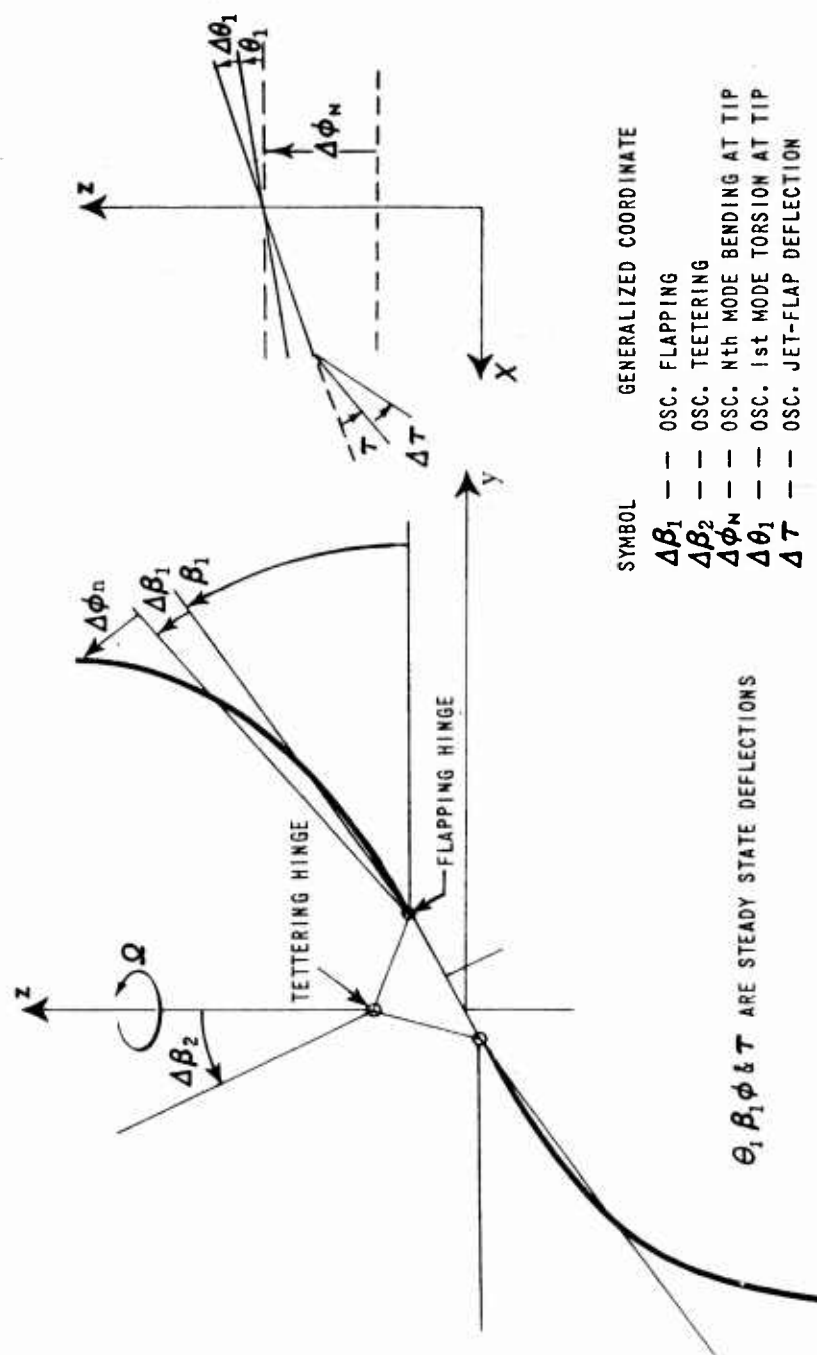


Figure 5. SCHEMATIC REPRESENTATION OF TWO BLADED JET-FLAP ROTOR

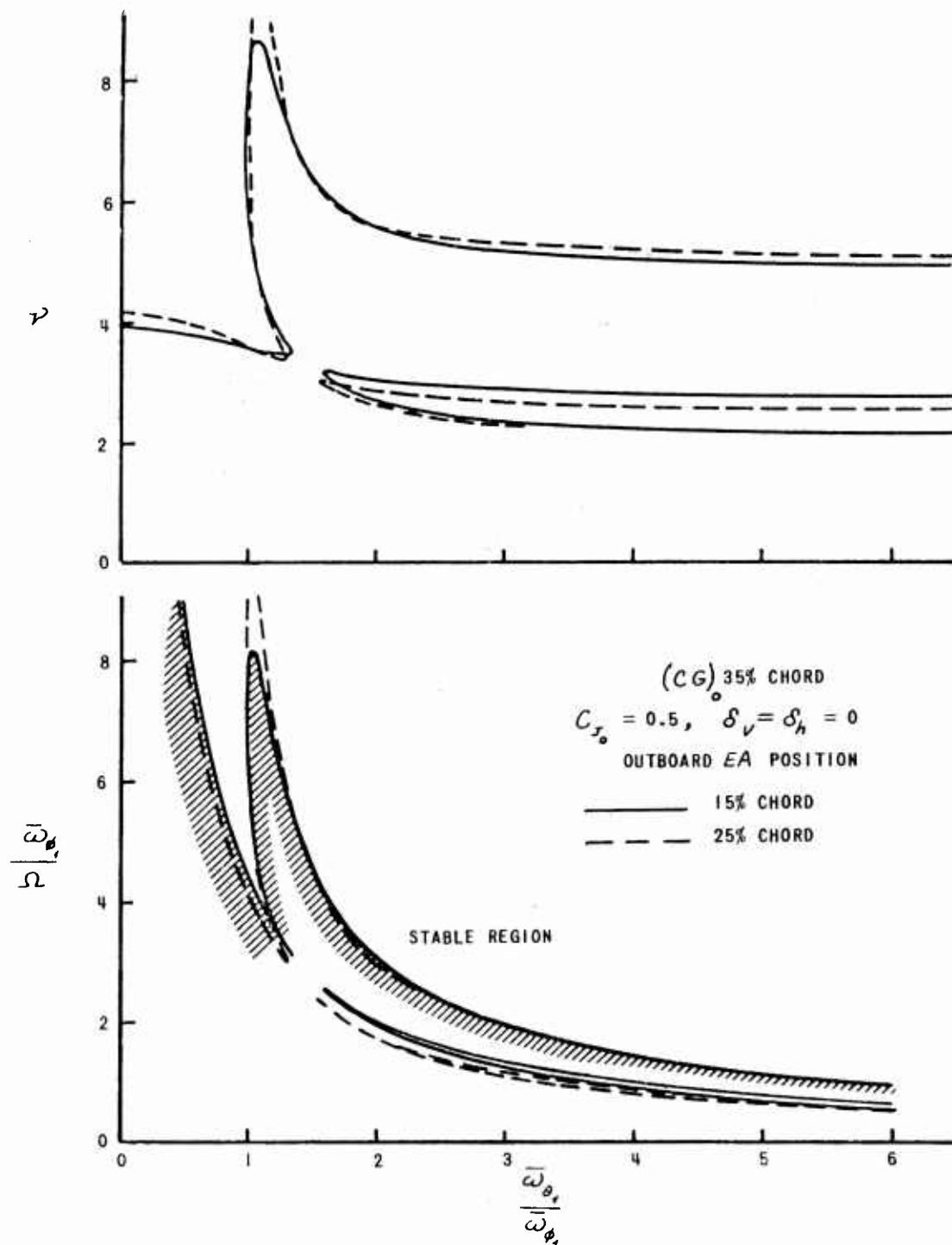


Figure 6. COMPARISON OF ν AND $\frac{\bar{\omega}_{\phi_1}}{\Omega}$ vs $\frac{\omega_{\theta_1}}{\omega_{\phi_1}}$ FOR DIFFERENT ELASTIC AXIS POSITION

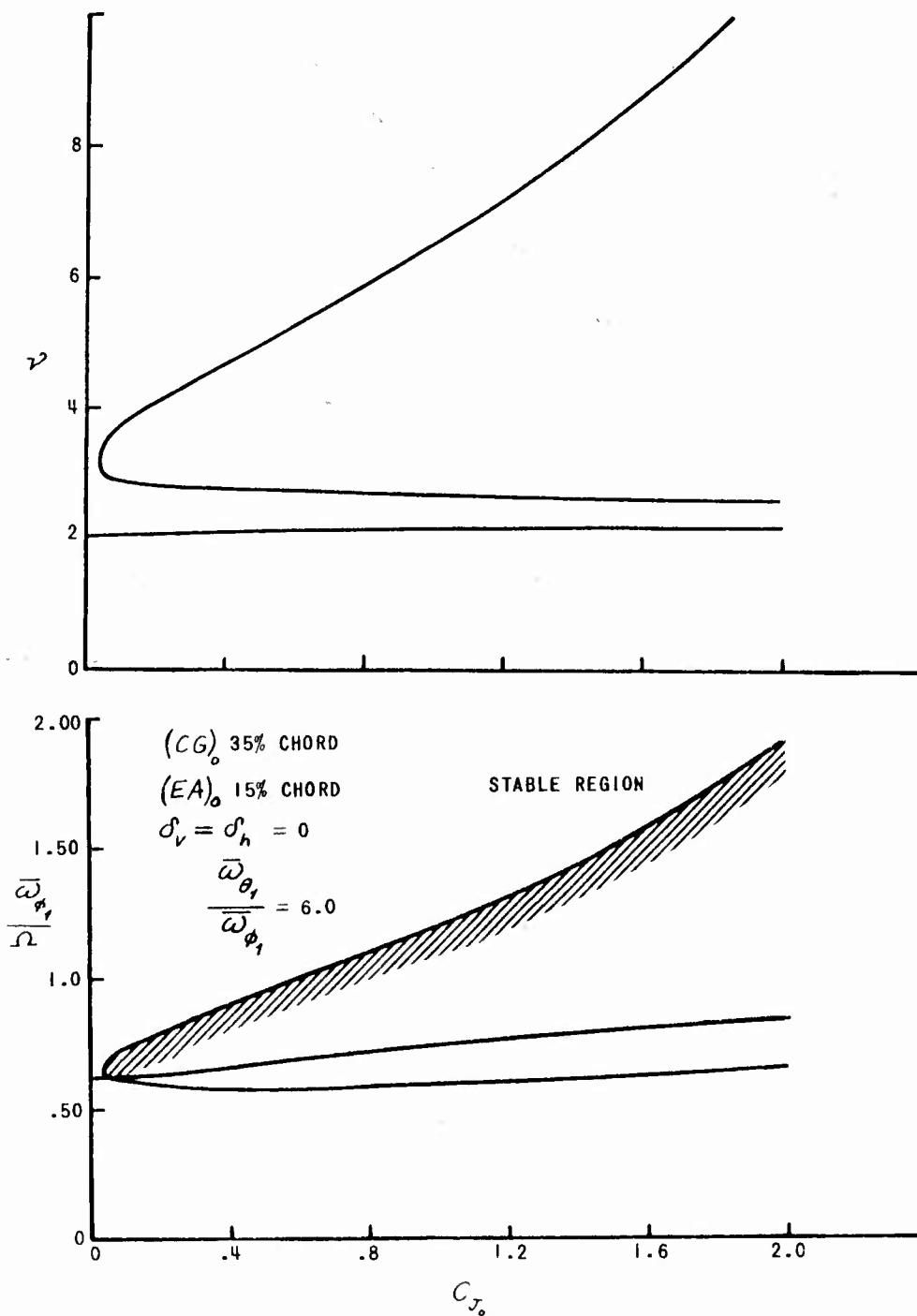


Figure 7. ν AND $\frac{\bar{\omega}_{\phi_1}}{\Omega}$ vs JET BLOWING COEFFICIENT C_{J_0} .

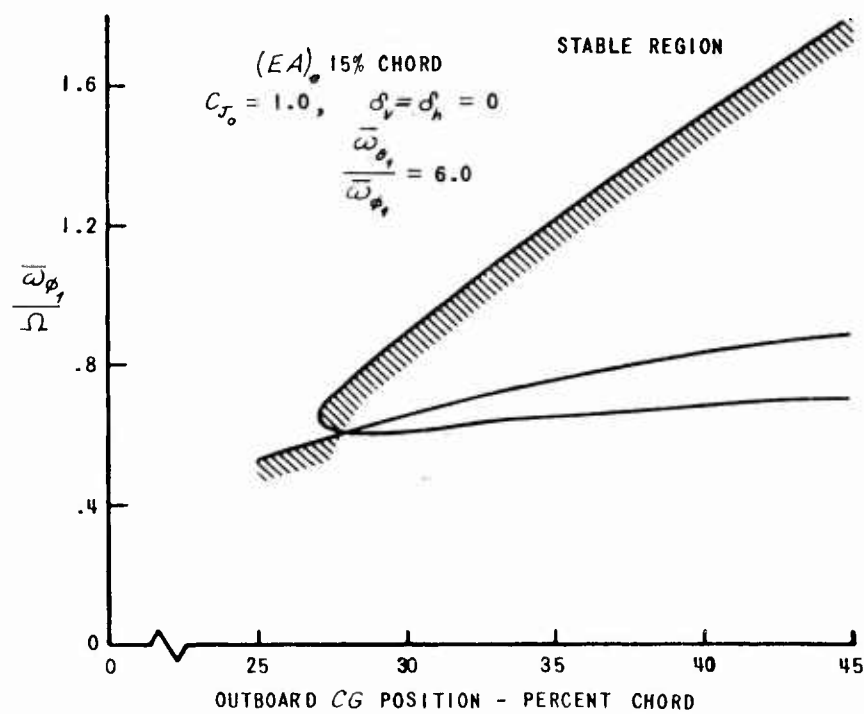
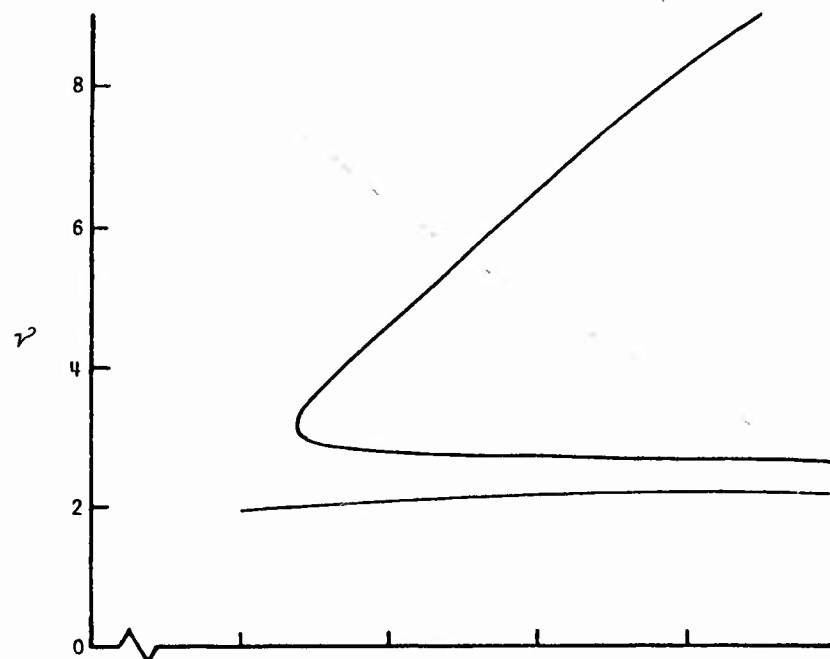


Figure 8. r^2 AND $\frac{\bar{\omega}_{\phi_1}}{\Omega}$ vs OUTBOARD CG POSITION

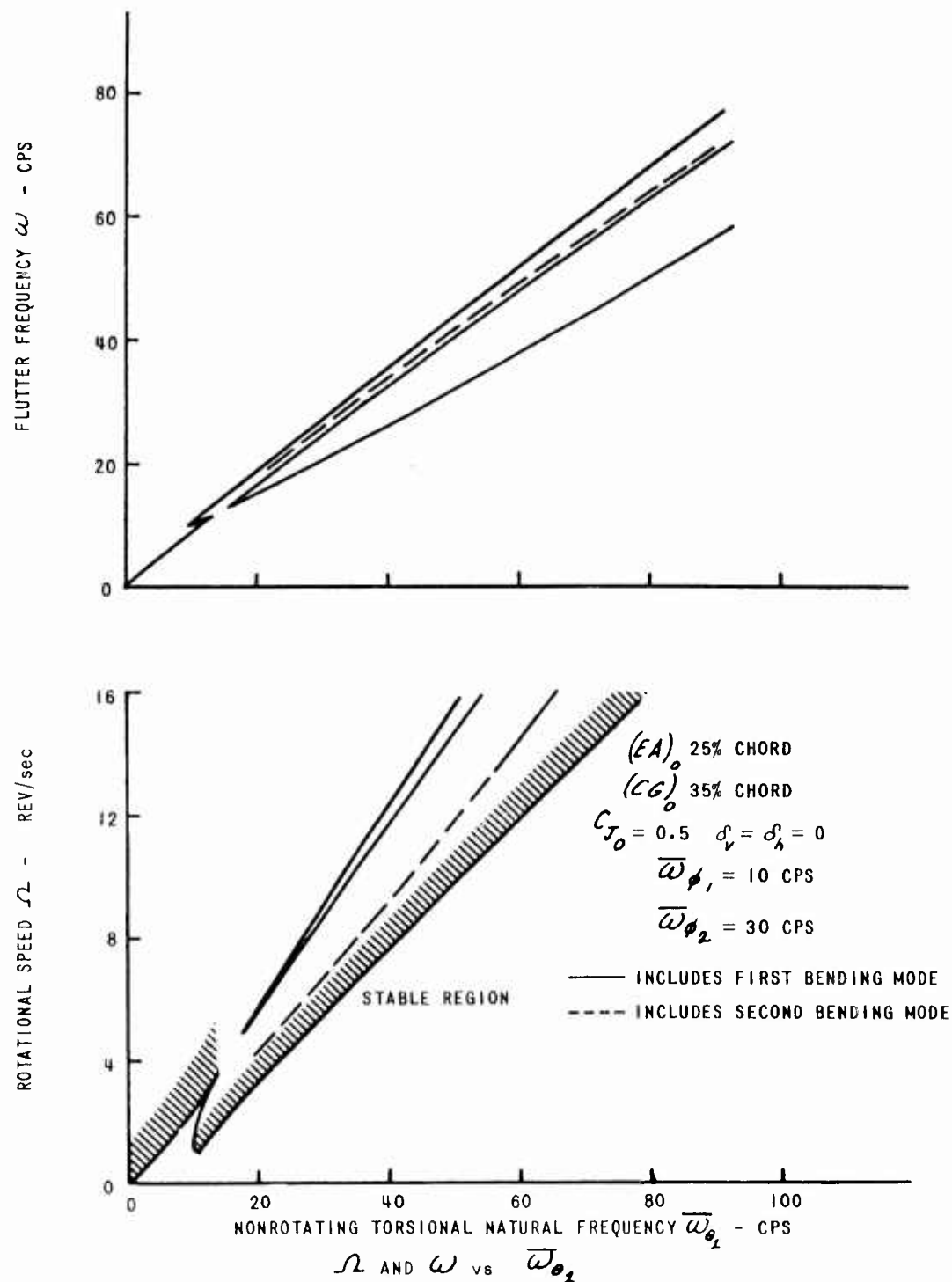


Figure 9. COMPARISON OF EFFECTS OF FIRST AND SECOND BENDING MODES

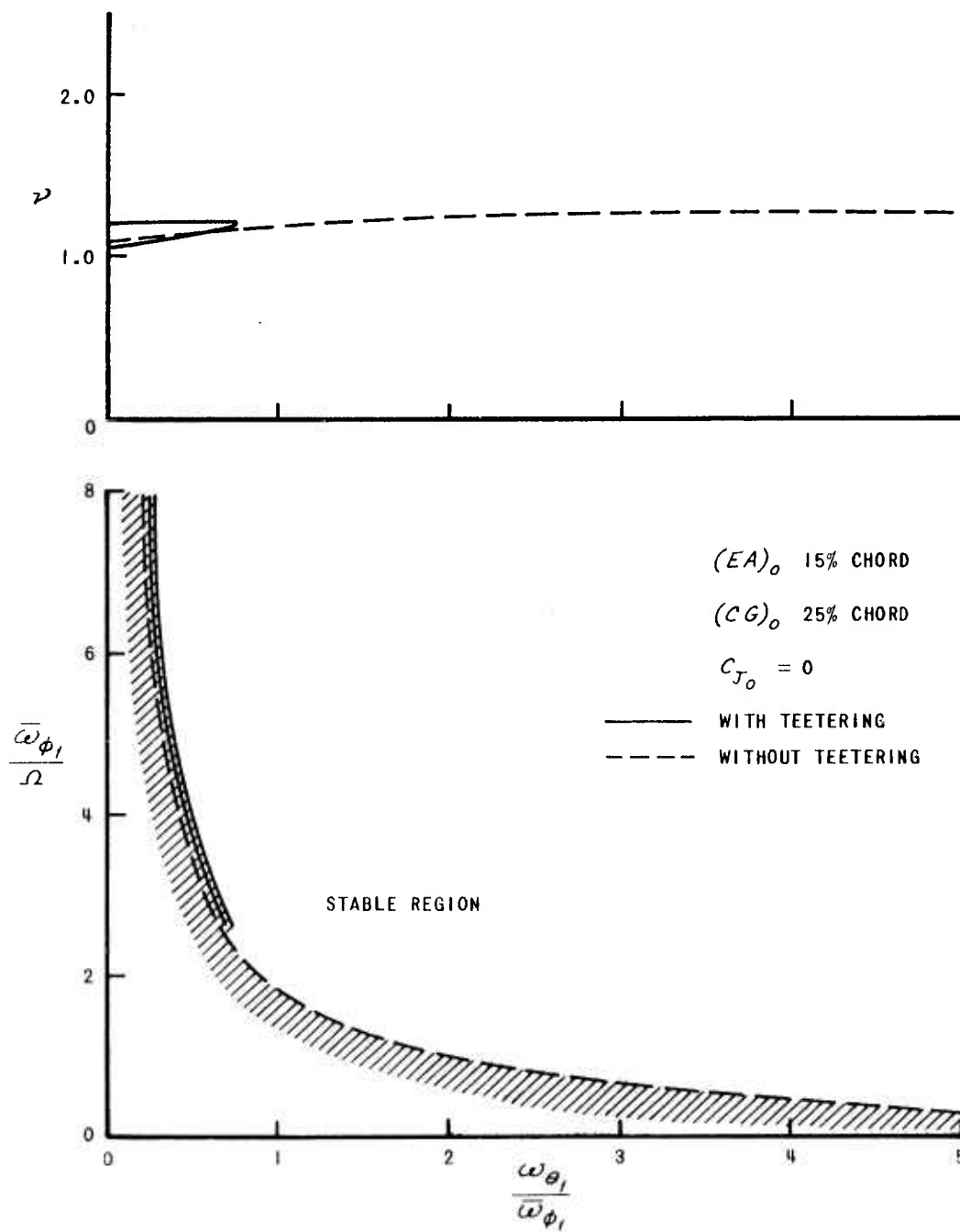


Figure 10. COMPARISON OF ν AND $\frac{\bar{\omega}_{\phi_1}}{\Omega}$ vs $\frac{\bar{\omega}_{\theta_1}}{\bar{\omega}_{\phi_1}}$ WITH AND WITHOUT TEETERING $C_{J_o} = 0$

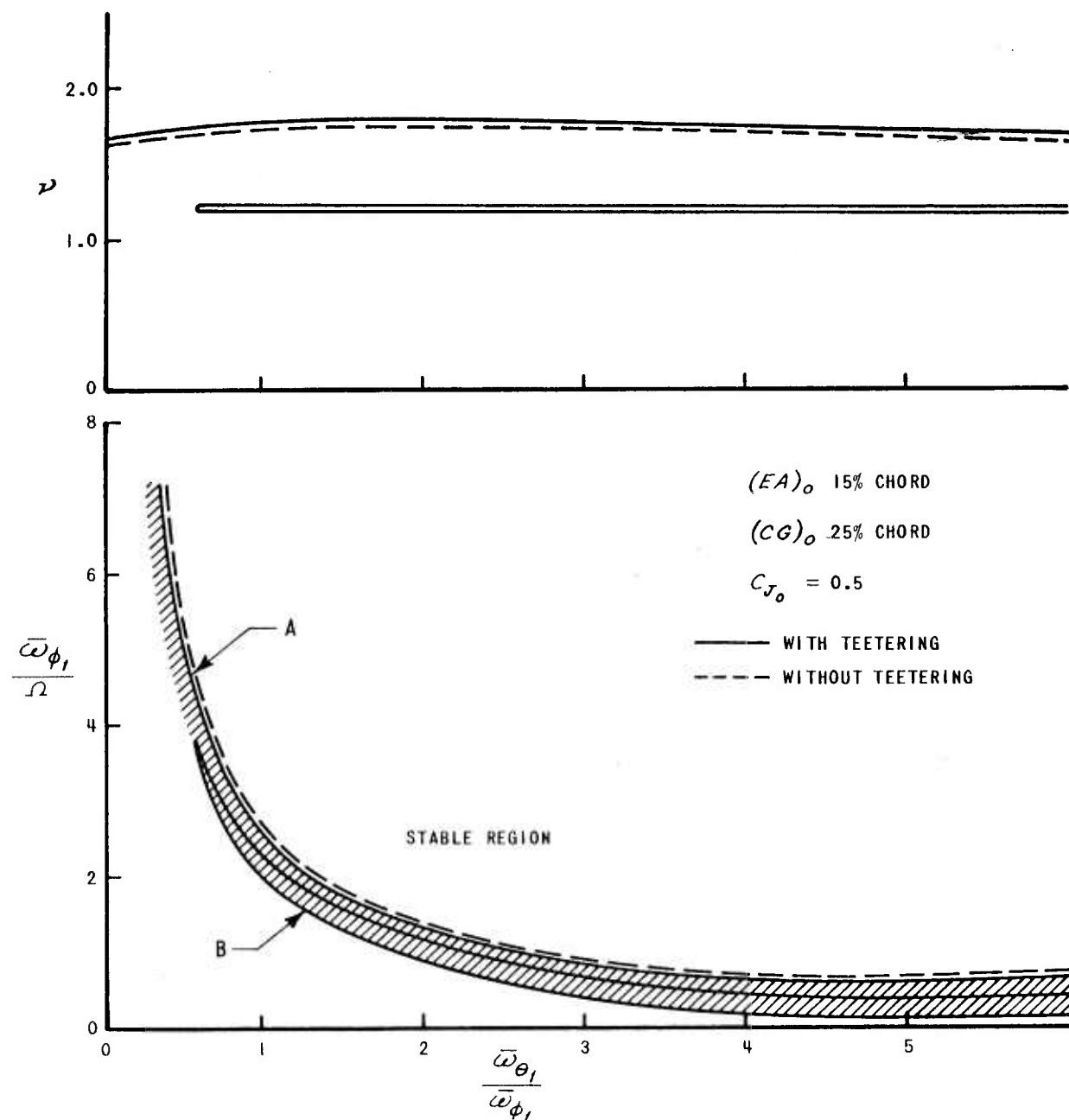


Figure 11. COMPARISON OF ν AND $\frac{\bar{\omega}_{\phi_1}}{\Omega}$ vs $\frac{\bar{\omega}_{\theta_1}}{\bar{\omega}_{\phi_1}}$ WITH AND WITHOUT TEETERING $C_{J_o} = 0.5$

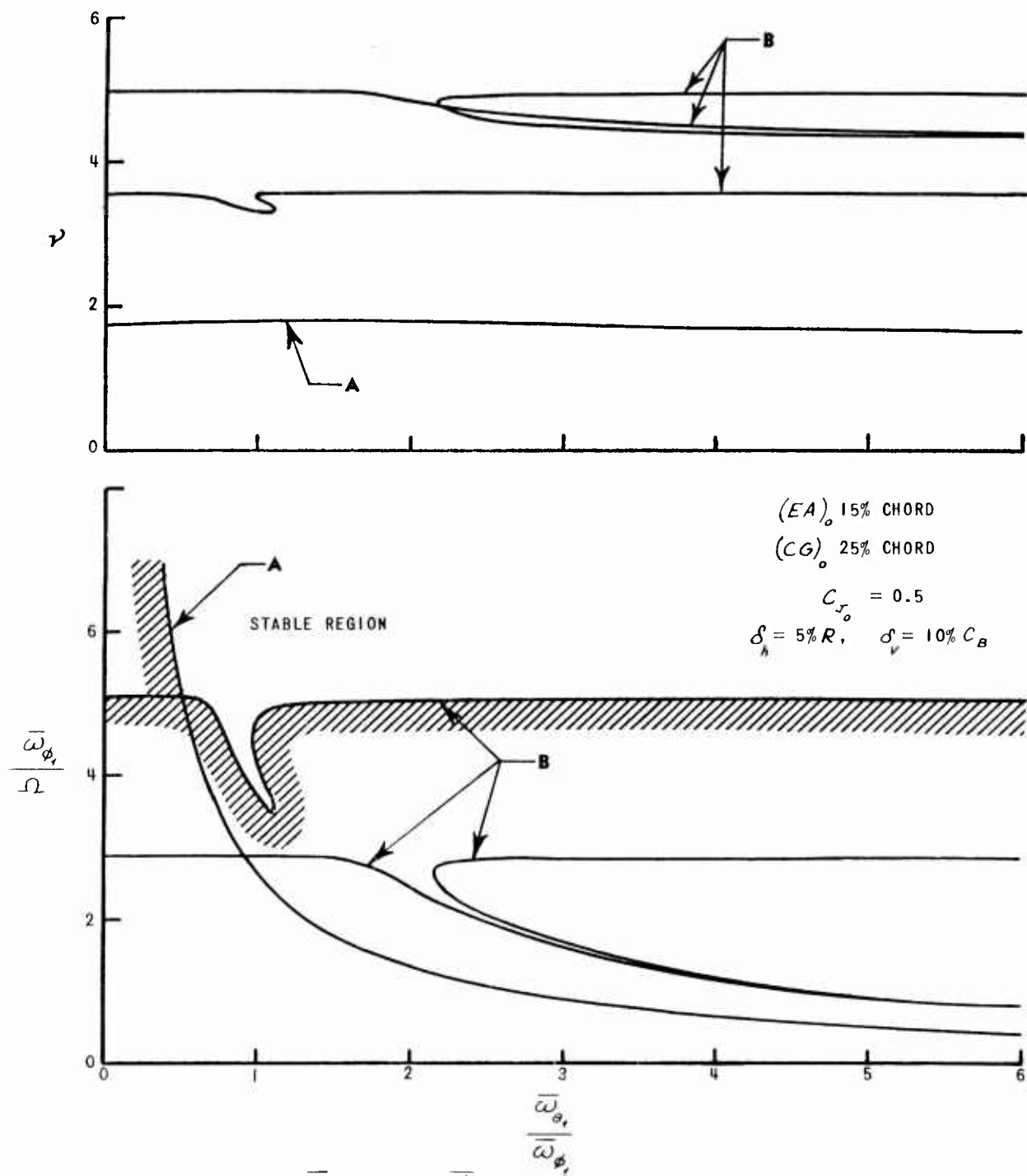


Figure 12. ν AND $\frac{\bar{\omega}_{\phi_1}}{\Omega}$ vs $\frac{\bar{\omega}_{\theta_1}}{\bar{\omega}_{\phi_1}}$ FOR OFFSET ROTOR - CG AT 25% CHORD

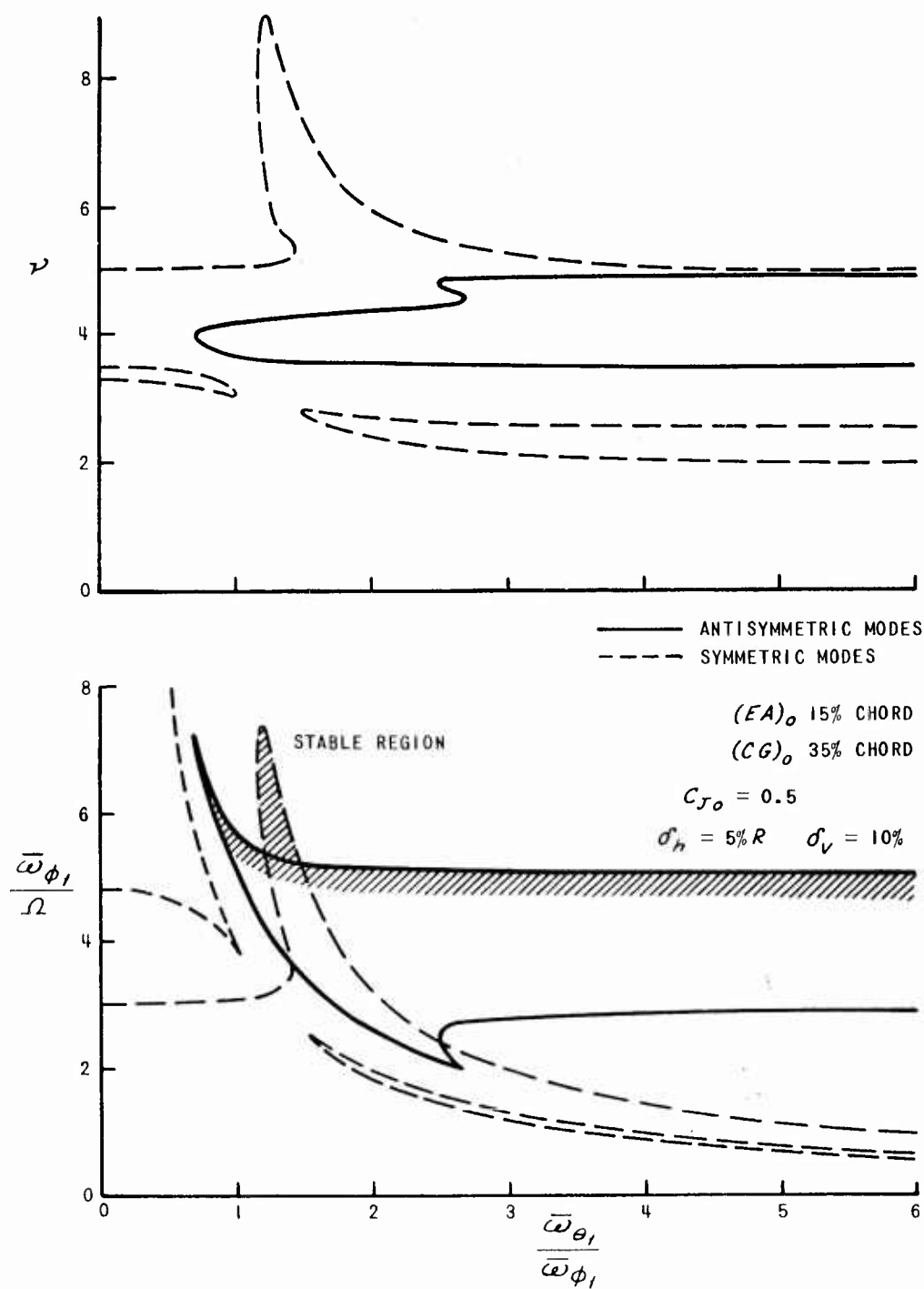


Figure 13. ζ AND $\frac{\bar{\omega}_{\phi_1}}{\Omega}$ vs $\frac{\bar{\omega}_{\theta_1}}{\bar{\omega}_{\phi_1}}$ FOR OFFSET ROTOR - CG AT 35% CHORD

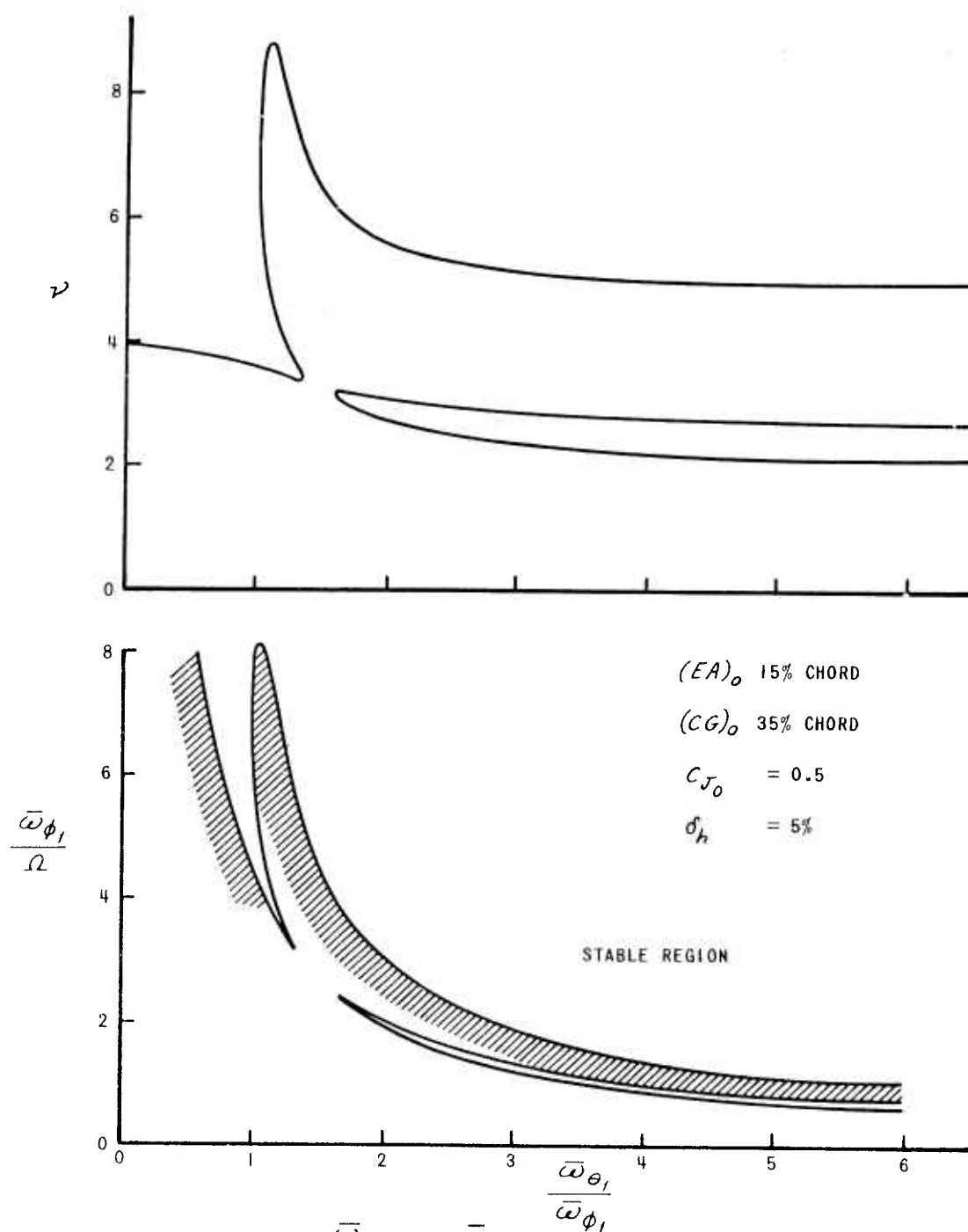


Figure 14. ν AND $\frac{\bar{\omega}_{\phi_1}}{\Omega}$ vs $\frac{\bar{\omega}_{\theta_1}}{\bar{\omega}_{\phi_1}}$ FOR OFFSET ROTOR - NO TEETERING

V. BIBLIOGRAPHY

1. DuWaldt, F. A., Gates, C. A., and Piziali, R. A. "Investigation of Helicopter Rotor Blade Flutter and Flapwise Bending Response in Hovering", WADC Technical Report 59-403, August, 1959
2. Daughaday, H., DuWaldt, F., and Gates, C., "Investigation of Helicopter Rotor Flutter and Load Amplification Problems", Journal of the American Helicopter Society, Vol. 2, No. 3, July, 1957
3. Daughaday, H., "Flutter Analysis of the H-5 Rotor with a Pitch-Cone Coupling Linkage", Cornell Aeronautical Laboratory Report No. BB-538-S-3, July, 1952
4. Brooks, G., and Becker, H., "An Experimental Investigation of the Effects of Various Parameters Including Tip Mach Number on the Flutter of Some Model Helicopter Rotor Blades", NACARM L53D24, June, 1953
5. Miller, R., and Ellis, C., "Helicopter Blade Vibration and Flutter", I.A.S. Preprint No. 635, January, 1956
6. Chan, P., "Pitch-Lag Instability of Helicopter Rotors", Journal of the American Helicopter Society, Vol. 3, No. 3, July 1958
7. Zvara, J., "The Aeroelastic Stability of Helicopter Rotors in Hovering Flight", Aeroelastic and Structures Research Laboratory, M.I.T. Technical Report 61-1, September, 1956
8. Timman, R., and van de Vooren, A., "Flutter of a Helicopter Rotor Rotating in its Own Wake", National Aeronautical Research Institute, Report No. Fl87, Amsterdam, April, 1956
9. Dorand, Rene, and Boehler, F. D., "Application of the Jet-Flap Principle to Helicopters", Paper presented before the American Helicopter Society Fifteenth Annual National Forum, Washington, D. C., May 7-9, 1959

V. BIBLIOGRAPHY (Continued)

10. Dorand, Rene, and Torarine, S., "Design Study of the Feasibility of Flying-Crane Type Helicopters Incorporating the Jet-Flap Control System", Engineering Division-Giravions Dorand, For the European Research Office, U. S. Department of the Army Report No. 1088, 30 April 1959 (Volume I and II)
11. Loewy, R. "A Two-Dimensional Approximation to the Unsteady Aerodynamics of Rotary Wings", Cornell Aeronautical Report No. 75, October, 1955 Also, Journal of Aeronautical Sciences Vol. 24, No. 2, February 1957
12. Targoff, Walter P., "The Bending Vibrations of a Twisted Rotating Beam", WADC Technical Report 56-27, December, 1955
13. Daughaday, H., DuWaldt, F., Gates, C., "Investigation of Helicopter Rotor Flutter and Load Amplification Problems", Cornell Aeronautical Report No. SB-862-S-4, August, 1956
14. Hough, G. R., "Cambered Jet-Flap Airfoil Theory" Masters Thesis, Cornell University, September, 1959
15. Spence, D. A., "The Theory of the Jet-Flap for Unsteady Motion", Journal of Fluid Mechanics, Vol. 10, Part 2, March, 1961

LIST OF SYMBOLS FOR APPENDICES

A_{ij}	generalized aerodynamic force coefficient
a_{ij}	real part of flutter determinant element
B	tip loss factor
b_{ij}	imaginary part of flutter determinant element
b	local semichord
b_{ref}	reference length - maximum semichord length
\bar{b}_f	nondimensional local flap semichord - $\bar{b}_f = \frac{b_f}{b}$
C_L	two-dimensional lift coefficient
C_M	two-dimensional moment coefficient, referred to the aerodynamic moment about the leading edge, positive nose down
C_J	jet coefficient $C_J = \frac{\rho_f V_f^2 \delta_f}{\rho U^2 b}$
C_{J_0}	value of C_J at $\bar{E} = 1$
\bar{C}_x	nondimensional distance of section c.g. position aft of elastic axis - $\bar{C}_x = \bar{x}_1/b$
\bar{C}_z	nondimensional distance of section c.g. position above chord plane - $\bar{C}_z = \bar{z}_1/b$
\bar{C}_{fx}	nondimensional distance from blade elastic axis to flap c.g. $\bar{C}_{fx} = \bar{x}_{f1}/b$

LIST OF SYMBOLS FOR APPENDICES (Continued)

f_{ϕ_n}	bending deflection shape - n^{th} mode, unit tip deflection
$f_{\phi_n}^* \Delta \phi_n$	perturbation bending displacement referred to root chord plane - $f_{\phi_n}^* \Delta \phi_n = f_{\phi_n} \Delta \phi_n - r \left(\frac{df_{\phi_n}}{dr} \right)_{r=0} \Delta \phi_n$
f_{θ_1}	first cantilever torsional mode shape - unit tip deflection
G_{ij}	generalized gyroscopic coupling coefficient
g_i	structural damping coefficient for i^{th} degree of freedom
$\left. \begin{matrix} \bar{g} \\ \bar{h} \end{matrix} \right\}$	correction terms to account for warping of elastic axis in chord plane - $\bar{g} = 2 \int_0^{\xi} f_{\theta_1}(\xi_1) F(\xi_1) d\xi_1$
	$\bar{h} = \int_0^{\xi} F(\xi_1) d\xi_1, \text{ where } F(\xi_1) = \frac{df_{\theta_1}}{d\xi_1} \left[\bar{I}(\xi_1) - \frac{\epsilon_b(\xi_1)}{\epsilon_b(\xi)} \bar{I}(\xi_1) - \frac{(\xi - \xi_1)}{\epsilon_b(\xi)} \frac{d(\epsilon_b \bar{I})}{d\xi_1} \right]$
\bar{I}_{x_1}	nondimensional moment of inertia about elastic axis due to chordwise mass distribution - $\bar{I}_{x_1} = \frac{1}{M_b R^2} I_{x_1}$
\bar{I}_{z_1}	nondimensional moment of inertia about elastic axis due to mass distribution normal to chord plane - $\bar{I}_{z_1} = \frac{1}{M_b R^2} I_{z_1}$
$\bar{I}_{z_1, (root)}$	contribution to \bar{I}_{z_1} from part of root fitting which flaps
\bar{I}_{fx}	nondimensional moment of inertia of control flap about its leading edge due to chordwise mass distribution - $\bar{I}_{fx} = \frac{1}{M_b R^2} I_{fx}$
\bar{I}_{fz}	nondimensional moment of inertia of control flap about its leading edge due to mass distribution normal to chord plane - $\bar{I}_{fz} = \frac{1}{M_b R^2} I_{fz}$

LIST OF SYMBOLS FOR APPENDICES (Continued)

\bar{I}_H	nondimensional hub moment of inertia about teetering hinge - $\bar{I}_H = \frac{1}{M_b R^2} I_H$
K_{ij}	generalized stiffness coefficient
K_α	flap moment coefficient derivatives
$K_{\dot{\alpha}}$	
	M_f (flap leading edge) = $-2b_f^2 r U^2 \left[K_\alpha \alpha_f + K_{\dot{\alpha}} \left(\frac{b_f \dot{\alpha}_f}{U} \right) \right]$
	where α_f is flap local angle-of-attack
\bar{l}	nondimensional distance of elastic axis aft of pitching (reference) axis - $\bar{l} = l/b$
M_b	total mass of one blade
M_{ij}	generalized mass coefficient
M'	aerodynamic moment per unit span
\bar{m}	nondimensional mass per unit spanwise length, $\bar{m} = \frac{m R}{M_b}$
\bar{m}_f	nondimensional mass per unit spanwise length of the mechanical flap - $\bar{m}_f = \frac{m_f R}{M_b}$
\bar{Q}	nondimensional distance of aerodynamic reference axis (midchord) aft of elastic axis - $\bar{Q} = Q/b$
q_i	the i^{th} generalized coordinate
R	blade radius
r	spanwise distance from flapping hinge
r_o	inboard spanwise limit on integration of aerodynamic forces

LIST OF SYMBOLS FOR APPENDICES (Continued)

\bar{r}_o	nondimensional lower limit on aerodynamic spanwise integrals - $\bar{r}_o = r_o/R$
T_{ij}	generalized centrifugal force coefficient
t	maximum camber
U	local free stream velocity
V_j	magnitude of jet velocity relative to airfoil
W_o	average downwash velocity
X', Y', Z'	components of aerodynamic force per unit span in the $x, y,$ and z directions, respectively
(x, y, z)	coordinate system rotating at angular speed Ω , z axis aligned with $\underline{\Omega}$, positive y axis directed outward along blade
\bar{x}_f	nondimensional distance from control flap leading edge to elastic axis - $\bar{x}_f = x_f/b$
α	local angle of attack
β_i	initial flapping angle
$\Delta\beta_i$	perturbation flapping angle with respect to y axis
$\Delta\beta_2$	perturbation teetering angle of hub with respect to z axis
$\bar{\delta}_h$	nondimensional distance from center of rotation to flapping hinge - $\bar{\delta}_h = \delta_h/R$
$\bar{\delta}_v$	nondimensional vertical distance of teetering hinge above the flapping hinge - $\bar{\delta}_v = \delta_v/R$

LIST OF SYMBOLS FOR APPENDICES (Continued)

δ_J	jet thickness
ϵ_b	ratio of local semichord to reference semichord length
θ_0	pitch angle with respect to $x-y$ plane
θ_i	initial blade twist about elastic axis
$\Delta\theta_i$	perturbation torsional deflection at the blade tip about the elastic axis
μ	mass ratio, $\mu = \frac{M_b}{\rho b_{ref} R^2}$
ν	ratio of oscillation frequency to shaft rotational speed, $\nu = \frac{\omega}{\Omega}$
ξ	nondimensional spanwise coordinate, $\xi = \frac{r}{R}$
ξ_0	value of ξ defining length of jet-flap, flap is $(1-\xi_0)R$ long
ρ	density of the free stream
ρ_J	air density of the jet
τ	steady state jet angle with respect to mean chord line
$\Delta\tau$	perturbation jet deflection angle
$\bar{\phi}_i$	nondimensional initial bending deflection, $\bar{\phi}_i = \frac{\phi_i}{R}$

LIST OF SYMBOLS FOR APPENDICES (Continued)

$\Delta \bar{\phi}_n$	nondimensional perturbation bending displacement at blade tip in n^{th} natural mode - $\Delta \bar{\phi}_n = \frac{\Delta \phi_n}{R}$
Ω	rotational speed of the rotor
ω	oscillation frequency
$\bar{\omega}_i$	uncoupled, undamped, nonrotating, natural frequency of i^{th} degree of freedom

APPENDIX I

DERIVATION OF FLUTTER DETERMINANT ELEMENTS

A. GENERAL EQUATIONS OF MOTION

The general equations of motion for a helicopter blade are derived, using the Lagrangian approach, as in Appendix I of Reference 13. The resulting relationship for the i^{th} degree of freedom ($i = 1, 2, \dots, N$) assuming the system is undergoing sinusoidal motions at a frequency ω , may be written as follows:

$$(I.1) \quad \sum_{j=1}^N \left(-\omega^2 M_{ij} + K_{ij} - \Omega^2 T_{ij} - 2i\omega \Omega G_{ij} - \Omega^2 A_{ij} \right) q_j = 0$$

The q_j 's are the generalized coordinates, and the quantities M_{ij} , T_{ij} and G_{ij} may be identified as the generalized mass, centrifugal force, and gyroscopic coupling coefficients, respectively. These coefficients are given by the following integrals over the entire system.

$$M_{ij} = \iiint \left[\left(\frac{\partial x}{\partial q_i} \right)_0 \left(\frac{\partial x}{\partial q_j} \right)_0 + \left(\frac{\partial y}{\partial q_i} \right)_0 \left(\frac{\partial y}{\partial q_j} \right)_0 + \left(\frac{\partial z}{\partial q_i} \right)_0 \left(\frac{\partial z}{\partial q_j} \right)_0 \right] dm$$

$$T_{ij} = \iiint \left[\left(\frac{\partial x}{\partial q_i} \right)_0 \left(\frac{\partial x}{\partial q_j} \right)_0 + \left(\frac{\partial y}{\partial q_i} \right)_0 \left(\frac{\partial y}{\partial q_j} \right)_0 + x_0 \left(\frac{\partial^2 x}{\partial q_i \partial q_j} \right)_0 + y_0 \left(\frac{\partial^2 y}{\partial q_i \partial q_j} \right)_0 \right] dm$$

$$G_{ij} = \iiint \left[\left(\frac{\partial x}{\partial q_i} \right)_0 \left(\frac{\partial y}{\partial q_j} \right)_0 - \left(\frac{\partial y}{\partial q_i} \right)_0 \left(\frac{\partial x}{\partial q_j} \right)_0 \right] dm$$

where (x , y , z) are the coordinates of the differential mass dm , referred to a rotating orthogonal coordinate system having the z - axis aligned with the angular velocity Ω and the positive y axis directed outward along the blade. The subscript (0) refers to the value of that quantity when all perturbations on the generalized coordinates are zero. The generalized spring forces K_{ij} are given by

$$K_{ij} = \left(\frac{\partial^2 \mathcal{U}}{\partial q_i \partial q_j} \right)_0$$

APPENDIX I (Continued)

where \mathcal{U} is the total potential energy of the system. The generalized aerodynamic force coefficients A_{ij} were derived from consideration

of the generalized (nonconservative) forces acting on the system, and are given by the following integrals over the spanwise variable r .

$$A_{ij} = \frac{1}{\Omega^2} \int_{r_0}^{BR} \left[\left(\frac{\partial x}{\partial q_i} \right)_0 \left(\frac{\partial \Delta x'}{\partial q_j} \right) + \left(\frac{\partial y}{\partial q_i} \right)_0 \left(\frac{\partial \Delta y'}{\partial q_j} \right) + \left(\frac{\partial z}{\partial q_i} \right)_0 \left(\frac{\partial \Delta z'}{\partial q_j} \right) + \left(\frac{\partial \eta}{\partial q_i} \right)_0 \left(\frac{\partial \Delta M'}{\partial q_j} \right) \right. \\ \left. + (x')_0 \left(\frac{\partial^2 x}{\partial q_i \partial q_j} \right) + (y')_0 \left(\frac{\partial^2 y}{\partial q_i \partial q_j} \right) + (z')_0 \left(\frac{\partial^2 z}{\partial q_i \partial q_j} \right) + (M')_0 \left(\frac{\partial^2 \eta}{\partial q_i \partial q_j} \right) \right] dr$$

where $[(x')_0 + \Delta x']$, etc., are the aerodynamic forces per unit span in the x , y and z directions, respectively. $[(M')_0 + \Delta M']$ is the aerodynamic moment per unit span corresponding to the angular displacement η , and B is the tip correction factor.

B. FORMULATION OF THE ELEMENTS OF THE FLUTTER DETERMINANT

Each of the generalized coefficients appearing in the equations of motion was computed, in a manner analogous to the one described in Reference 13, using the aerodynamic coefficients derived in APPENDIX I where applicable. The generalized coordinates considered in the generation of these coefficients are:

- β_1 - blade flapping angle with respect to y -axis
- β_2 - hub teetering angle with respect to z -axis
- $\bar{\phi}_n = \frac{\phi_n}{R}$ - nondimensionalized n^{th} mode bending displacement at blade tip
- θ_1 - first mode torsional deflection at blade tip
- τ - jet angle with respect to mean chord line

So that the formulation of the problem would be more general, the equations of motion were nondimensionalized by dividing through by the quantity $\rho b_{ref} \Omega^2 R^4$. The nondimensionalized coefficients are

APPENDIX I (Continued)

given by

$$\begin{aligned}\bar{M}_{ij} &= \frac{M_{ij}}{\rho b_{ref} R^4} & \bar{A}_{ij} &= \frac{A_{ij}}{\rho b_{ref} R^4} \\ \bar{T}_{ij} &= \frac{T_{ij}}{\rho b_{ref} R^4} & \bar{K}_{ij} &= \frac{K_{ij}}{\rho b_{ref} R^4 \Omega^2} \\ \bar{G}_{ij} &= \frac{G_{ij}}{\rho b_{ref} R^4}\end{aligned}$$

The ij^{th} element of the flutter determinant, with real and imaginary parts designated by a_{ij} and b_{ij} , respectively, are therefore given by:

$$\left\{ \begin{aligned} a_{ij} &= -v^2 \bar{M}_{ij} + \bar{K}_{ij} - \bar{T}_{ij} - \mathcal{R}\{\bar{A}_{ij}\} \\ b_{ij} &= -2v \bar{G}_{ij} - \mathcal{I}\{\bar{A}_{ij}\} \end{aligned} \right\} \quad i \neq j$$

$$\left\{ \begin{aligned} a_{ii} &= \left(-v^2 + \frac{\bar{\omega}_i^2}{\Omega^2} \right) \bar{M}_{ii} - \bar{T}_{ii} - \mathcal{R}\{\bar{A}_{ii}\} \\ b_{ii} &= -2v \bar{G}_{ii} + g_i \frac{\omega_i^2}{\Omega^2} \bar{M}_{ii} - \mathcal{I}\{\bar{A}_{ii}\} \end{aligned} \right\} \quad i = j$$

The expressions for the nondimensional coefficients making up these elements are given on the following pages. It should be noted that an additional factor of 2 is applied to all $i \beta_2$ coefficients. This factor actually should be included in the definition of the determinant elements $i \beta_2$, because the teetering vibrations are excited only when the two blades of the rotor exhibit antisymmetric oscillations. The factor of 2 thus appears when the seven-degree-of-freedom system is reduced to one with four degrees of freedom. The factor was applied to the coefficients instead, however, to simplify the definition of the determinant elements.

APPENDIX I (Continued)

Generalized Mass Coefficients

$$\bar{M}_{\phi_n \phi_n} = \mu \left[\int_0^1 (f_{\phi_n})^2 \bar{m} d\bar{\epsilon} + \left(\frac{df_{\phi_n}}{d\bar{\epsilon}} \right)_{\bar{\epsilon}=0}^2 \bar{I}_{z, (root)} \right]$$

$$\bar{M}_{\phi_n \theta_1} = -\mu \frac{b_{ref}}{R} \int_0^1 \epsilon_b f_{\phi_n} \bar{m} (f_{\theta_1} \bar{c}_x + \bar{h}) d\bar{\epsilon}$$

$$\bar{M}_{\phi_n \beta_1} = -\mu \int_0^1 \bar{\epsilon} f_{\phi_n} \bar{m} d\bar{\epsilon}$$

$$\bar{M}_{\phi_n \beta_2} = 2\mu \bar{\delta}_h \int_0^1 f_{\phi_n} \bar{m} d\bar{\epsilon}$$

$$\bar{M}_{\phi_n \tau} = -\mu \frac{b_{ref}}{R} \int_{\bar{\epsilon}_0}^1 \epsilon_b f_{\phi_n} (\bar{c}_{fx} - \bar{x}_f) \bar{m}_f d\bar{\epsilon}$$

$$\bar{M}_{\theta_1 \phi_n} = \bar{M}_{\phi_n \theta_1}$$

$$\bar{M}_{\theta_1 \theta_1} = \mu \int_0^1 \left\{ f_{\theta_1}^2 \left[\frac{d\bar{I}_{zz}}{d\bar{\epsilon}} + \frac{d\bar{I}_{xz_1}}{d\bar{\epsilon}} \right] + \bar{m} \epsilon_b^2 \left(\frac{b_{ref}}{R} \right)^2 \bar{h} \left[\bar{h} + 2\bar{c}_x f_{\theta_1} \right] \right\} d\bar{\epsilon}$$

$$\bar{M}_{\theta_1 \beta_1} = -\mu \frac{b_{ref}}{R} \int_0^1 \epsilon_b \bar{\epsilon} \bar{m} (f_{\theta_1} \bar{c}_x + \bar{h}) d\bar{\epsilon}$$

$$\bar{M}_{\theta_1 \beta_2} = -2\mu \bar{\delta}_h \frac{b_1}{R} \int_0^1 \epsilon_b \bar{m} (f_{\theta_1} \bar{c}_x + \bar{h}) d\bar{\epsilon}$$

$$\bar{M}_{\theta_1 \tau} = \mu \int_{\bar{\epsilon}_0}^1 f_{\theta_1} \left[\frac{d\bar{I}_{fx}}{d\bar{\epsilon}} + \frac{d\bar{I}_{fz}}{d\bar{\epsilon}} + \bar{m}_f \epsilon_b^2 \left(\frac{b_{ref}}{R} \right)^2 \bar{x}_f (\bar{c}_{fx} - \bar{x}_f) \right] d\bar{\epsilon}$$

APPENDIX I (Continued)

Generalized Mass Coefficients (continued)

$$\bar{M}_{\beta_1 \phi_n} = \bar{M}_{\phi_n \beta_1}$$

$$\bar{M}_{\beta_1 \theta_1} = \bar{M}_{\theta_1 \beta_1}$$

$$\bar{M}_{\beta_1 \beta_1} = \mu \left[\int_0^1 \bar{m} \xi^2 d\xi + \bar{I}_{z_1}(\text{root}) \right]$$

$$\bar{M}_{\beta_1 \beta_2} = 2\mu \bar{\delta}_h \int_0^1 \xi \bar{m} d\xi$$

$$\bar{M}_{\beta_1 \tau} = -\mu \frac{b_{ref}}{R} \int_{\xi_0}^1 \epsilon_b \xi (\bar{c}_{fx} - \bar{x}_f) \bar{m}_f d\xi$$

$$\bar{M}_{\beta_2 \phi_n} = \frac{1}{2} \bar{M}_{\phi_n \beta_2}$$

$$\bar{M}_{\beta_2 \theta_1} = \frac{1}{2} \bar{M}_{\theta_1 \beta_2}$$

$$\bar{M}_{\beta_2 \beta_1} = \frac{1}{2} \bar{M}_{\beta_1 \beta_2}$$

$$\bar{M}_{\beta_2 \beta_2} = \mu \left[\bar{I}_H + 2(\bar{\delta}_v^2 + \bar{\delta}_h^2) \right]$$

$$\bar{M}_{\beta_2 \tau} = -\mu \bar{\delta}_h \frac{b_{ref}}{R} \int_{\xi_0}^1 \epsilon_b (\bar{c}_{fx} - \bar{x}_f) \bar{m}_f d\xi$$

APPENDIX I (Continued)

Generalized Mass Coefficients (continued)

$$\overline{M}_{\tau\phi_n} = \overline{M}_{\phi_n\tau}$$

$$\overline{M}_{\tau\theta_1} = \overline{M}_{\theta_1\tau}$$

$$\overline{M}_{\tau\beta_1} = \overline{M}_{\beta_1\tau}$$

$$\overline{M}_{\tau\beta_2} = 2\overline{M}_{\beta_2\tau}$$

$$\overline{M}_{\tau\tau} = \mu \int_{\xi_0}^1 \left(\frac{d\bar{I}_{fx}}{d\xi} + \frac{d\bar{I}_{fz}}{d\xi} \right) d\xi$$

Generalized Centrifugal Force Coefficients

$$\overline{T}_{\phi_n\phi_n} = \mu \left[- \int_0^1 \left(\frac{df_{\phi_n}}{d\xi} \right)^2 \left(\int_{\xi_0}^1 \bar{m} d\xi_1 \right) d\xi + \left(\frac{df_{\phi_n}}{d\xi} \right)_{\xi_0=0}^2 \bar{I}_z(\text{root}) \right]$$

$$\overline{T}_{\phi_n\theta_1} = \mu \frac{b_{ref}}{R} \int_0^1 \epsilon_b \xi \frac{df_{\phi_n}}{d\xi} \bar{m} (f_{\theta_1} \bar{c}_x + \bar{h}) d\xi$$

$$\overline{T}_{\phi_n\beta_1} = -\mu \int_0^1 f_{\phi_n} (\xi + \bar{\delta}_n) \bar{m} d\xi$$

$$\overline{T}_{\phi_n\beta_2} = -2\mu \bar{\delta}_v \int_0^1 \left[\int_0^{\xi} \frac{d\bar{\phi}_1}{d\xi_1} \frac{df_{\phi_n}}{d\xi_1} + \epsilon_b \frac{b_{ref}}{R} \bar{c}_z \frac{df_{\phi_n}}{d\xi} + f_{\phi_n} \beta_1 \right] \bar{m} d\xi$$

APPENDIX I (Continued)

Generalized Centrifugal Force Coefficients (continued)

$$\overline{T}_{\phi_n, x} = \mu \frac{b_{ref}}{R} \int_{\xi_0}^1 \epsilon_b \xi \frac{d f_{\phi_n}}{d \xi} \left(\overline{C}_{fx} - \overline{x}_f \right) \overline{m}_f d \xi$$

$$\overline{T}_{\phi_n, \phi_1} = \overline{T}_{\phi_n, \theta_1}$$

$$\overline{T}_{\theta, \theta_1} = \mu \int_0^1 \left\{ f_{\theta_1}^2 \left[\frac{d \overline{I}_{z_1}}{d \xi} - \frac{d \overline{I}_{x_1}}{d \xi} \right] - \epsilon_b^2 \left(\frac{b_{ref}}{R} \right)^2 \overline{m} \left[f_{\theta_1}^2 \overline{C}_x \overline{I} + (\overline{I} + \overline{C}_x) \overline{g} \right] \right\} d \xi$$

$$\overline{T}_{\theta, \beta_1} = \mu \frac{b_{ref}}{R} \int_0^1 \epsilon_b \xi \overline{m} \left(f_{\theta_1} \overline{C}_x + \overline{h} \right) d \xi$$

$$\overline{T}_{\theta, \beta_2} = 2 \mu \overline{\delta}_v \frac{b_{ref}}{R} \int_0^1 \left(\frac{d \overline{\phi}_1}{d \xi} + \beta_1 \right) \left(f_{\theta_1} \overline{C}_x + \overline{h} \right) \overline{m} d \xi$$

$$\overline{T}_{\theta, x} = \mu \int_{\xi_0}^1 f_{\theta_1} \left\{ \frac{d \overline{I}_{fx}}{d \xi} - \frac{d \overline{I}_{fx}}{d \xi} + \overline{m}_f \left(\frac{b_{ref}}{R} \right)^2 \epsilon_b^2 \left[\overline{x}_f \left(\overline{x}_f + \overline{I} - \overline{C}_{fx} \right) - \overline{I} \overline{C}_{fx} \right] \right\} d \xi$$

$$\overline{T}_{\beta_1, \phi_n} = \overline{T}_{\phi_n, \beta_1}$$

$$\overline{T}_{\beta_1, \theta} = \overline{T}_{\theta, \beta_1}$$

$$\overline{T}_{\beta_1, \beta_1} = \mu \left[\overline{I}_{z_1, (root)} - \int_0^1 \xi \left(\xi + \overline{\delta}_h \right) \overline{m} d \xi \right]$$

$$\overline{T}_{\beta_1, \beta_2} = -2 \mu \overline{\delta}_v \int_0^1 \left(\beta_1 \xi + \frac{b_{ref}}{R} \epsilon_b \overline{C}_x + \overline{\phi}_1 \right) \overline{m} d \xi$$

APPENDIX I (Continued)

Generalized Centrifugal Force Coefficients (continued)

$$\bar{T}_{\beta_1 \tau} = \mu \frac{b_{ref}}{R} \int_{\xi_0}^1 \epsilon_b \xi \left(\bar{c}_{fx} - \bar{x}_f \right) \bar{m}_f d\xi$$

$$\bar{T}_{\beta_2 \phi_n} = \frac{1}{2} \bar{T}_{\phi_n \beta_2}$$

$$\bar{T}_{\beta_2 \theta_1} = \frac{1}{2} \bar{T}_{\theta_1 \beta_2}$$

$$\bar{T}_{\beta_2 \beta_1} = \frac{1}{2} \bar{T}_{\beta_1 \beta_2}$$

$$\bar{T}_{\beta_2 \beta_2} = \mu \left\{ \frac{1}{M_b R^2} \int_{Hub} \left[\left(\delta_v - z \right)^2 - y^2 \right] dm + 2 \left(\bar{\delta}_v^2 - \bar{\delta}_h^2 \right) - 2 \bar{\delta}_h \int_0^1 \xi \bar{m} d\xi \right\}$$

$$\bar{T}_{\beta_2 \tau} = \mu \bar{\delta}_v \frac{b_{ref}}{R} \int_{\xi_0}^1 \epsilon_b \left(\frac{d \bar{\phi}_1}{d \xi} + \beta_1 \right) \left(\bar{c}_{fx} - \bar{x}_f \right) \bar{m}_f d\xi$$

$$\bar{T}_{\tau \phi_n} = \bar{T}_{\phi_n \tau}$$

$$\bar{T}_{\tau \theta_1} = \bar{T}_{\theta_1 \tau}$$

$$\bar{T}_{\tau \beta_1} = \bar{T}_{\beta_1 \tau}$$

$$\bar{T}_{\tau \beta_2} = 2 \bar{T}_{\beta_2 \tau}$$

APPENDIX I (Continued)

Generalized Centrifugal Force Coefficients (continued)

$$\bar{T}_{\epsilon\epsilon} = \mu \int_{\epsilon_0}^{\epsilon_1} \left\{ \frac{d\bar{I}_{fz}}{d\epsilon} - \frac{d\bar{I}_{fz}}{d\epsilon} + \bar{m}_f \left(\frac{b_{ref}}{R} \right)^2 \epsilon_b^2 \left[\bar{x}_f (\bar{x}_f + \bar{l} - \bar{c}_{fx}) - \bar{l} \bar{c}_{fx} \right] \right\} d\epsilon$$

Generalized Gyroscopic Coupling Coefficients

$$G_{ij} \equiv 0, \quad i = j$$

$$\bar{G}_{\phi_n \theta_1} = 0$$

$$\bar{G}_{\phi_n \beta_1} = -\mu \int_0^1 (\bar{\phi}_1 + \beta_1 \epsilon) f_{\phi_n}^* \theta_0 \bar{m} d\epsilon$$

$$\bar{G}_{\phi_n \beta_2} = 2\mu \bar{\delta}_v \int_0^1 f_{\phi_n}^* \theta_0 \bar{m} d\epsilon$$

$$\bar{G}_{\phi_n x} = 0$$

$$\bar{G}_{\theta_1 \phi_n} = 0$$

$$\bar{G}_{\theta_1 \beta_1} = -\mu \int_0^1 f_{\theta_1} \frac{d\bar{I}_{x_1}}{d\epsilon} d\epsilon$$

$$\bar{G}_{\theta_1 \beta_2} = -2\mu \bar{\delta}_v \frac{b_{ref}}{R} \int_0^1 \epsilon_b f_{\theta_1} \bar{c}_x (\theta_0 + \theta_1) \bar{m} d\epsilon$$

APPENDIX I (Continued)

Generalized Gyroscopic Coupling Coefficients (continued)

$$\bar{G}_{\theta, \tau} = 0$$

$$\bar{G}_{\beta, \phi_n} = -\bar{G}_{\phi_n, \beta_1}$$

$$\bar{G}_{\beta, \theta_1} = -\bar{G}_{\theta_1, \beta_1}$$

$$\bar{G}_{\beta, \beta_2} = 0$$

$$\bar{G}_{\beta, \tau} = 0$$

$$\bar{G}_{\beta_2, \phi_n} = -\frac{1}{2} \bar{G}_{\phi_n, \beta_2}$$

$$\bar{G}_{\beta_2, \theta_1} = -\frac{1}{2} \bar{G}_{\theta_1, \beta_2}$$

$$\bar{G}_{\beta_2, \beta_1} = 0$$

$$\bar{G}_{\beta_2, \tau} = 0$$

$$\bar{G}_{\tau, \phi_n} = 0$$

APPENDIX I (Continued)

Generalized Gyroscopic Coupling Coefficients (continued)

$$\bar{G}_{r\theta_1} = 0$$

$$\bar{G}_{r\beta_1} = 0$$

$$\bar{G}_{r\beta_2} = 0$$

Generalized Stiffness Coefficients

$$\bar{K}_{ij} = 0, \quad i \neq j$$

$$\bar{K}_{\phi_n \phi_n} = \frac{1}{\rho b_{ref} R^5 \Omega^2} \int_0^1 EI \left(\frac{d^2 f_{\phi_n}}{d\xi^2} \right)^2 d\xi \equiv \bar{M}_{\phi_n \phi_n} \frac{\bar{\omega}_{\phi_n}^2}{\Omega^2}$$

$$\bar{K}_{\theta_1 \theta_1} = \frac{1}{\rho b_{ref} R \Omega^2} \int_0^1 GJ \left(\frac{df_{\theta_1}}{d\xi} \right)^2 d\xi \equiv \bar{M}_{\theta_1 \theta_1} \frac{\bar{\omega}_{\theta_1}^2}{\Omega^2}$$

$$\bar{K}_{\beta_1 \beta_1} = 0$$

$$\bar{K}_{\beta_2 \beta_2} = 0$$

$$\bar{K}_{rr} \equiv \bar{M}_{rr} \frac{\bar{\omega}_r^2}{\Omega^2}$$

APPENDIX I (Continued)

Generalized Aerodynamic Force Coefficients

$$\bar{A}_{\phi_n \phi_n} = \frac{b_{ref}}{R} \int_{\bar{r}_0}^B \epsilon_b^2 \xi f_{\phi_n} \frac{d f_{\phi_n}}{d \xi} \left[\frac{1}{4} \frac{\partial C_L}{\partial (\psi/2b)} + (\bar{l} + \bar{Q}) \left(\frac{\partial C_L}{\partial \alpha} - C_L \right) \right] d \xi$$

$$- i v \int_{\bar{r}_0}^B \epsilon_b \xi f_{\phi_n}^2 \left(\frac{\partial C_L}{\partial \alpha} - C_J \right) d \xi$$

$$\bar{A}_{\phi_n \theta_1} = \int_{\bar{r}_0}^B \epsilon_b \xi^2 f_{\phi_n} f_{\theta_1} \frac{\partial C_L}{\partial \alpha} d \xi + i v \frac{b_{ref}}{R} \int_{\bar{r}_0}^B \epsilon_b^2 \xi^2 f_{\phi_n} \left[\frac{f_{\theta_1}}{4} \frac{\partial C_L}{\partial (\psi/2b)} \right.$$

$$\left. + (f_{\theta_1} \bar{Q} + \bar{h}) \left(\frac{\partial C_L}{\partial \alpha} - C_J \right) \right] d \xi$$

$$\bar{A}_{\phi_n \beta_1} = \frac{b_{ref}}{R} \int_{\bar{r}_0}^B \epsilon_b^2 \xi f_{\phi_n} \left[\frac{1}{4} \frac{\partial C_L}{\partial (\psi/2b)} + (\bar{l} + \bar{Q}) \left(\frac{\partial C_L}{\partial \alpha} - C_J \right) \right] d \xi$$

$$- i v \int_{\bar{r}_0}^B \epsilon_b \xi^2 f_{\phi_n} \left(\frac{\partial C_L}{\partial \alpha} - C_J \right) d \xi$$

$$\bar{A}_{\phi_n \beta_2} = -2 i v \bar{\delta}_h \int_{\bar{r}_0}^B \epsilon_b \xi f_{\phi_n} \left(\frac{\partial C_L}{\partial \alpha} - C_J \right) d \xi$$

$$\bar{A}_{\phi_n \tau} = \int_{\bar{r}_0}^B \epsilon_b \xi^2 f_{\phi_n} \frac{\partial C_L}{\partial \tau} d \xi + i v \frac{b_{ref}}{R} \int_{\bar{r}_0}^B \epsilon_b^2 \xi f_{\phi_n} \frac{\partial C_L}{\partial \tau} d \xi$$

$$\bar{A}_{\theta_1 \phi_n} = - \left(\frac{b_{ref}}{R} \right)^2 \int_{\bar{r}_0}^B \epsilon_b^3 \xi \frac{d f_{\phi_n}}{d \xi} \left\{ 2 f_{\theta_1} \left[\frac{1}{4} \left(\frac{\partial C_M}{\partial (\psi/2b)} - \frac{1}{2} \frac{\partial C_L}{\partial (\psi/2b)} \right) + (\bar{l} + \bar{Q}) \left(\frac{\partial C_M}{\partial \alpha} - \frac{1}{2} \frac{\partial C_L}{\partial \alpha} \right) \right] \right.$$

$$\left. + (f_{\theta_1} \bar{Q} + \bar{h}) \left[\frac{1}{4} \frac{\partial C_L}{\partial (\psi/2b)} + (\bar{l} + \bar{Q}) \left(\frac{\partial C_L}{\partial \alpha} - C_J \right) \right] \right\} d \xi$$

$$+ i v \frac{b_{ref}}{R} \int_{\bar{r}_0}^B \epsilon_b^2 \xi f_{\phi_n} \left[2 f_{\theta_1} \left(\frac{\partial C_M}{\partial \alpha} - \frac{1}{2} \frac{\partial C_L}{\partial \alpha} \right) + (f_{\theta_1} \bar{Q} + \bar{h}) \left(\frac{\partial C_L}{\partial \alpha} - C_J \right) \right] d \xi$$

APPENDIX I (Continued)

Generalized Aerodynamic Force Coefficients (continued)

$$\begin{aligned}\bar{A}_{\theta, \theta_1} = & -\frac{b_{ref}}{R} \int_{\bar{r}_0}^B \epsilon_b^2 \xi^2 \left[2f_{\theta_1}^2 \left(\frac{\partial C_M}{\partial \alpha} - \frac{1}{2} \frac{\partial C_L}{\partial \alpha} \right) + \left(f_{\theta_1}^2 \bar{Q} + \bar{g} \right) \left(\frac{\partial C_L}{\partial \alpha} - C_J \right) \right] d\xi \\ & - i\nu \left(\frac{b_{ref}}{R} \right) \int_{\bar{r}_0}^B \epsilon_b^3 \xi \left\{ 2f_{\theta_1} \left[\frac{f_{\theta_1}}{4} \left(\frac{\partial C_M}{\partial (t/2b)} - \frac{1}{2} \frac{\partial C_L}{\partial (t/2b)} \right) + \left(f_{\theta_1} \bar{Q} + \bar{h} \right) \left(\frac{\partial C_M}{\partial \alpha} - \frac{1}{2} \frac{\partial C_L}{\partial \alpha} \right) \right] \right. \\ & \left. + \left(f_{\theta_1} \bar{Q} + \bar{h} \right) \left[\frac{f_{\theta_1}}{4} \frac{\partial C_L}{\partial (t/2b)} + \left(f_{\theta_1} \bar{Q} + \bar{h} \right) \left(\frac{\partial C_L}{\partial \alpha} - C_J \right) \right] \right\} d\xi\end{aligned}$$

$$\begin{aligned}\bar{A}_{\theta, \beta_1} = & -\left(\frac{b_{ref}}{R} \right) \int_{\bar{r}_0}^B \epsilon_b^3 \xi \left\{ 2f_{\theta_1} \left[\frac{1}{4} \left(\frac{\partial C_M}{\partial (t/2b)} - \frac{1}{2} \frac{\partial C_L}{\partial (t/2b)} \right) + \left(\bar{l} + \bar{Q} \right) \left(\frac{\partial C_M}{\partial \alpha} - \frac{1}{2} \frac{\partial C_L}{\partial \alpha} \right) \right] \right. \\ & \left. + \left(f_{\theta_1} \bar{Q} + \bar{h} \right) \left[\frac{1}{4} \frac{\partial C_L}{\partial (t/2b)} + \left(\bar{l} + \bar{Q} \right) \left(\frac{\partial C_L}{\partial \alpha} - C_J \right) \right] \right\} d\xi \\ & + i\nu \frac{b_{ref}}{R} \int_{\bar{r}_0}^B \epsilon_b^2 \xi^2 \left[2f_{\theta_1} \left(\frac{\partial C_M}{\partial \alpha} - \frac{1}{2} \frac{\partial C_L}{\partial \alpha} \right) + \left(f_{\theta_1} \bar{Q} + \bar{h} \right) \left(\frac{\partial C_L}{\partial \alpha} - C_J \right) \right] d\xi\end{aligned}$$

$$\bar{A}_{\theta, \beta_2} = -2i\nu \frac{b_{ref}}{R} \bar{\delta}_h \int_{\bar{r}_0}^B \epsilon_b^2 \xi \left[2f_{\theta_1} \left(\frac{\partial C_M}{\partial \alpha} - \frac{1}{2} \frac{\partial C_L}{\partial \alpha} \right) + \left(f_{\theta_1} \bar{Q} + \bar{h} \right) \left(\frac{\partial C_L}{\partial \alpha} - C_J \right) \right] d\xi$$

$$\begin{aligned}\bar{A}_{\theta, \tau} = & -\frac{b_{ref}}{R} \int_{\bar{r}_0}^B \epsilon_b^2 \xi^2 f_{\theta_1} \left[2 \left(\frac{\partial C_M}{\partial \tau} - \frac{1}{2} \frac{\partial C_L}{\partial \tau} \right) + \bar{Q} \frac{\partial C_L}{\partial \tau} \right] d\xi \\ & - i\nu \left(\frac{b_{ref}}{R} \right)^2 \int_{\bar{r}_0}^B \epsilon_b^3 \xi f_{\theta_1} \left[2 \left(\frac{\partial C_M}{\partial \tau} - \frac{1}{2} \frac{\partial C_L}{\partial \tau} \right) + \bar{Q} \frac{\partial C_L}{\partial \tau} \right] d\xi\end{aligned}$$

$$\bar{A}_{\beta, \phi_n} = \frac{b_{ref}}{R} \int_{\bar{r}_0}^B \epsilon_b^2 \xi^2 \frac{df_{\phi_n}}{d\xi} \left[\frac{1}{4} \frac{\partial C_L}{\partial (t/2b)} + \left(\bar{l} + \bar{Q} \right) \left(\frac{\partial C_L}{\partial \alpha} - C_J \right) \right] d\xi - i\nu \int_{\bar{r}_0}^B \epsilon_b^2 \xi^2 f_{\theta_1} \left(\frac{\partial C_L}{\partial \alpha} - C_J \right) d\xi$$

APPENDIX I (Continued)

Generalized Aerodynamic Force Coefficients (continued)

$$\bar{A}_{\beta_1 \theta_1} = \int_{\frac{r_0}{\bar{r}_0}}^B \epsilon_b \bar{\xi}^3 f_{\theta_1} \frac{\partial C_L}{\partial \alpha} d\bar{\xi} + i\nu \frac{b_{ref}}{R} \int_{\frac{r_0}{\bar{r}_0}}^B \epsilon_b^2 \bar{\xi}^2 \left[\frac{f_{\theta_1}}{4} \frac{\partial C_L}{\partial (t/2b)} + (f_{\theta_1} \bar{Q} + \bar{h}) \left(\frac{\partial C_L}{\partial \alpha} - C_T \right) \right] d\bar{\xi}$$

$$\bar{A}_{\beta_1 \beta_1} = \frac{b_{ref}}{R} \int_{\frac{r_0}{\bar{r}_0}}^B \epsilon_b^2 \bar{\xi}^2 \left[\frac{1}{4} \frac{\partial C_L}{\partial (t/2b)} + (\bar{l} + \bar{Q}) \left(\frac{\partial C_L}{\partial \alpha} - C_T \right) \right] d\bar{\xi} - i\nu \int_{\frac{r_0}{\bar{r}_0}}^B \epsilon_b \bar{\xi}^3 \left(\frac{\partial C_L}{\partial \alpha} - C_T \right) d\bar{\xi}$$

$$\bar{A}_{\beta_1 \beta_2} = -2 i\nu \bar{\delta}_h \int_{\frac{r_0}{\bar{r}_0}}^B \epsilon_b \bar{\xi}^2 \left(\frac{\partial C_L}{\partial \alpha} - C_T \right) d\bar{\xi}$$

$$\bar{A}_{\beta_1 \tau} = \int_{\frac{r_0}{\bar{r}_0}}^B \epsilon_b \bar{\xi}^3 \frac{\partial C_L}{\partial \tau} d\bar{\xi} + i\nu \frac{b_{ref}}{R} \int_{\frac{r_0}{\bar{r}_0}}^B \epsilon_b^2 \bar{\xi}^2 \frac{\partial C_L}{\partial \tau} d\bar{\xi}$$

$$\begin{aligned} \bar{A}_{\beta_2 \phi_n} = & \int_{\frac{r_0}{\bar{r}_0}}^B \epsilon_b \bar{\xi} \frac{d f_{\phi_n}}{d \bar{\xi}} \left\{ \bar{\delta}_h \epsilon_b \frac{b_{ref}}{R} \left[\frac{1}{4} \frac{\partial C_L}{\partial (t/2b)} + (\bar{l} + \bar{Q}) \left(\frac{\partial C_L}{\partial \alpha} - C_T \right) \right] \right. \\ & \left. - \bar{\delta}_v \bar{\xi} \left[\frac{\partial C_L}{\partial \alpha} \left(\theta_0 + \theta_1 - \frac{W_0}{\Omega \bar{\xi} R} \right) + \frac{\partial C_L}{\partial \tau} \tau + \frac{\partial C_L}{\partial (t/2b)} \left(\frac{t}{2b} \right) \right] \right\} d\bar{\xi} \\ & - i\nu \bar{\delta}_h \int_{\frac{r_0}{\bar{r}_0}}^B \epsilon_b \bar{\xi} f_{\phi_n} \left(\frac{\partial C_L}{\partial \alpha} - C_T \right) d\bar{\xi} \end{aligned}$$

$$\bar{A}_{\beta_2 \theta_1} = \bar{\delta}_h \int_{\frac{r_0}{\bar{r}_0}}^B \epsilon_b \bar{\xi}^2 f_{\theta_1} \frac{\partial C_L}{\partial \alpha} d\bar{\xi} + i\nu \bar{\delta}_h \frac{b_{ref}}{R} \int_{\frac{r_0}{\bar{r}_0}}^B \epsilon_b^2 \bar{\xi} \left[\frac{f_{\theta_1}}{4} \frac{\partial C_L}{\partial (t/2b)} + (f_{\theta_1} \bar{Q} + \bar{h}) \left(\frac{\partial C_L}{\partial \alpha} - C_T \right) \right] d\bar{\xi}$$

$$\begin{aligned} \bar{A}_{\beta_2 \beta_1} = & \int_{\frac{r_0}{\bar{r}_0}}^B \epsilon_b \bar{\xi} \left\{ \bar{\delta}_h \epsilon_b \frac{b_{ref}}{R} \left[\frac{1}{4} \frac{\partial C_L}{\partial (t/2b)} + (\bar{l} + \bar{Q}) \left(\frac{\partial C_L}{\partial \alpha} - C_T \right) \right] \right. \\ & \left. - \bar{\delta}_v \bar{\xi} \left[\frac{\partial C_L}{\partial \alpha} \left(\theta_0 + \theta_1 - \frac{W_0}{\Omega \bar{\xi} R} \right) + \frac{\partial C_L}{\partial \tau} \tau + \frac{\partial C_L}{\partial (t/2b)} \left(\frac{t}{2b} \right) \right] \right\} d\bar{\xi} - i\nu \bar{\delta}_h \int_{\frac{r_0}{\bar{r}_0}}^B \epsilon_b \bar{\xi}^2 \left(\frac{\partial C_L}{\partial \alpha} - C_T \right) d\bar{\xi} \end{aligned}$$

APPENDIX I (Continued)

Generalized Aerodynamic Force Coefficients (continued)

$$\bar{A}_{\beta_2 \beta_2} = \bar{\delta}_v \int_{\bar{r}_0}^B \epsilon_b \xi^2 \left[\frac{\partial C_L}{\partial \alpha} \left(\theta_0 + \theta_1 - \frac{W_0}{\Omega R \xi} \right) + \frac{\partial C_L}{\partial \tau} \tau + \frac{\partial C_L}{\partial (t/2b)} \left(\frac{t}{2b} \right) + C_T \frac{W_0}{\Omega \xi R} \right] d\xi \\ - i v \bar{\delta}_h^2 \int_{\bar{r}_0}^B \epsilon_b \xi \left(\frac{\partial C_L}{\partial \alpha} - C_T \right) d\xi$$

$$\bar{A}_{\beta_2 \tau} = \bar{\delta}_h \int_{\bar{r}_0}^B \epsilon_b \xi^2 \frac{\partial C_L}{\partial \tau} d\xi + i v \frac{b_{ref}}{R} \bar{\delta}_h \int_{\bar{r}_0}^B \epsilon_b^2 \xi \frac{\partial C_L}{\partial \tau} d\xi$$

$$\bar{A}_{\tau \phi_n} = -2 \left(\frac{b_{ref}}{R} \right)^2 \int_{\xi_0}^B \epsilon_b^3 \bar{b}_f^2 \xi \frac{d\phi_n}{d\xi} \left[K_\alpha (\bar{l} + \bar{x}_f) + K_\alpha \bar{b}_f \right] d\xi \\ + 2 i v \frac{b_{ref}}{R} \int_{\xi_0}^B \epsilon_b^2 \bar{b}_f^2 \xi f_{\phi_n} K_\alpha d\xi$$

$$\bar{A}_{\tau \theta_1} = -2 \frac{b_{ref}}{R} \int_{\xi_0}^B \epsilon_b^2 \bar{b}_f^2 \xi^2 f_{\theta_1} K_\alpha d\xi - 2 i v \left(\frac{b_{ref}}{R} \right)^2 \int_{\xi_0}^B \epsilon_b^3 \bar{b}_f^2 \xi f_{\theta_1} \left(K_\alpha \bar{x}_f + K_\alpha \bar{b}_f \right) d\xi$$

$$\bar{A}_{\tau \beta_1} = -2 \left(\frac{b_{ref}}{R} \right)^2 \int_{\xi_0}^B \epsilon_b^3 \bar{b}_f^2 \xi \left[K_\alpha (\bar{l} + \bar{x}_f) + K_\alpha \bar{b}_f \right] d\xi + 2 i v \frac{b_{ref}}{R} \int_{\xi_0}^B \epsilon_b^2 \bar{b}_f^2 \xi^2 K_\alpha d\xi$$

$$\bar{A}_{\tau \beta_2} = 4 i v \bar{\delta}_h \frac{b_{ref}}{R} \int_{\xi_0}^B \epsilon_b^2 \bar{b}_f \xi K_\alpha d\xi$$

$$\bar{A}_{\tau \tau} = -2 \frac{b_{ref}}{R} \int_{\xi_0}^B \epsilon_b^2 \bar{b}_f^2 \xi^2 K_\alpha d\xi - 2 i v \left(\frac{b_{ref}}{R} \right)^2 \int_{\xi_0}^B \epsilon_b^3 \bar{b}_f^3 K_\alpha d\xi$$

APPENDIX II

DERIVATION OF QUASI-STEADY AERODYNAMIC COEFFICIENTS FOR A TWO-DIMENSIONAL JET-FLAP AIRFOIL

A. CONSTANT JET ANGLE

In Reference 14, the lift and moment coefficients for a zero-thickness two-dimensional jet-flap airfoil with parabolic camber are derived for the steady case. These coefficients may be expressed as in Eqs. I.1 and I.2 below.

$$(I.1) \quad C_L = \frac{\partial C_L}{\partial \tau} \tau + \frac{\partial C_L}{\partial \alpha} \alpha + \frac{\partial C_L}{\partial (t/2b)} \left(\frac{t}{2b} \right)$$

$$(I.2) \quad C_M = \frac{\partial C_M}{\partial \tau} \tau + \frac{\partial C_M}{\partial \alpha} \alpha + \frac{\partial C_M}{\partial (t/2b)} \left(\frac{t}{2b} \right)$$

where τ , α , t and b are, respectively, the angle of the jet with respect to the airfoil chordline, angle of attack, maximum camber and the airfoil semichord. The moment coefficient C_M is defined to be positive for a nose-down moment about the leading edge. The derivatives

$\frac{\partial C_L}{\partial \alpha}$, $\frac{\partial C_M}{\partial \alpha}$, etc., are functions only of the jet coefficient C_J ,

the latter quantity being defined by

$$C_J \equiv \frac{\rho_J V_J^2 \delta_J}{\frac{1}{2} \rho U^2 (2b)}$$

where $\rho_J V_J^2 \delta_J$ is the momentum flux of the jet per unit span and $\frac{1}{2} \rho U^2$

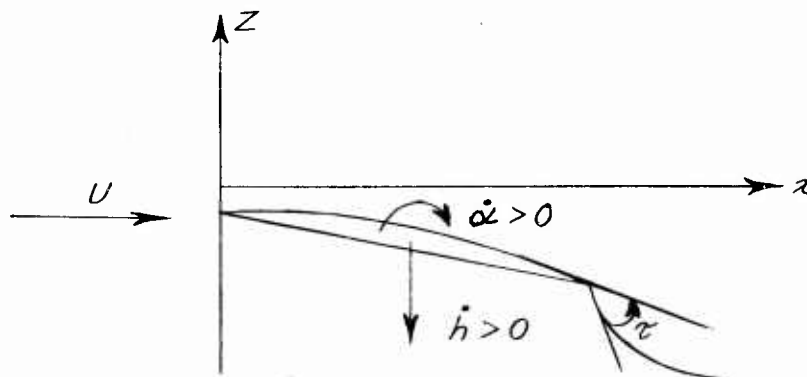
is the free stream dynamic pressure.

Consider the airfoil to be plunging at a rate \dot{h} , and pitching about

APPENDIX II (Continued)

A. CONSTANT JET ANGLE (continued)

midchord at a rate $\dot{\alpha}$, as sketched below



The plunging motion gives rise to a constant downwash across the airfoil which is equivalent under the quasi-steady assumption to an increase in angle of attack. The resulting total angle of attack is, thus, given by

$$\tilde{\alpha} = \alpha + \frac{\dot{h}}{U}$$

Similarly, the pitching motion produces a linearly varying downwash distribution over the airfoil, which is equivalent to a parabolic camber of the airfoil. It is easily shown that the effective camber is given by

$$\frac{\tilde{t}}{b} = \frac{t}{b} + \frac{b^2}{2U} \dot{\alpha}$$

The quasi-static approximations for the lift and moment coefficients are, therefore, given by the following expressions:

$$(II.3) \quad \frac{\tilde{L}}{C_L} = \frac{\partial C_L}{\partial \tau} \tau + \frac{\partial C_L}{\partial \alpha} \left(\alpha + \frac{\dot{h}}{U} \right) + \frac{\partial C_L}{\partial (t/2b)} \left(\frac{t}{2b} + \frac{b}{4U} \dot{\alpha} \right)$$

APPENDIX II (Continued)

A. CONSTANT JET ANGLE (continued)

$$(II.4) \quad \dot{C}_M = \frac{\partial C_M}{\partial \tau} \tau + \frac{\partial C_M}{\partial \alpha} \left(\alpha + \frac{\dot{h}}{U} \right) + \frac{\partial C_M}{\partial (t/2b)} \left(\frac{t}{2b} + \frac{b}{4U} \dot{\alpha} \right)$$

The above expressions were utilized in the flutter analysis by obtaining α , $\dot{\alpha}$ and \dot{h} in terms of the generalized coordinates chosen for the analysis, and substituting these relationships into Eqs. I.3 and I.4. Total lift and moment were then computed and applied to the calculation of generalized forces, as discussed in Appendix I.

B. OSCILLATING JET ANGLE

In Ref. 15, Spence analyzes the case of unsteady motion of the jet angle with respect to the airfoil chord line. He finds that if the reduced frequency is of order one or less and that $\frac{1}{4} C_j$ is much less than unity, the lift coefficient resulting from the jet is, in the first approximation, modified by a factor $\left(1 + i \frac{b}{R} \nu\right)$ where ν is the frequency of oscillation divided by the rotational speed. This factor was applied to the lift and moment derivatives with respect to τ when deriving the coefficients involving jet deflection.

The application of this factor to the moment coefficient is not strictly correct. It was learned through communication with Mr. J. Erickson that the factor applied to the moment coefficient should be

$\left(1 + i \frac{5}{4} \frac{b}{R} \nu\right)$. It was felt, however, that the error introduced by applying the same factor to both lift and moment coefficients could be tolerated to simplify computations.

DISTRIBUTION

USCONARC	(2)
First US Army	(1)
Second US Army	(1)
Third US Army	(1)
Fourth US Army	(1)
Fifth US Army	(1)
Sixth US Army	(2)
USA Infantry Center	(1)
USA Command & General Staff College	(1)
Army War College	(1)
USA Arctic Test Board	(1)
USA Cold Weather and Mountain School	(1)
USA Aviation School	(2)
USA Armor Board	(1)
USA Aviation Board	(2)
USA Aviation Test Office	(1)
Deputy Chief of Staff for Logistics, DA	(4)
Deputy Chief of Staff for Military Operations, DA	(1)
ORO, Johns Hopkins University	(1)
ARO, OCRD	(1)
Office of Chief of R&D, DA	(1)
ARO, Durham	(1)
USA Liaison Officer, Naval Air Test Center	(2)
USA Chemical Corps Board	(1)
USA Ordnance Missile Command	(1)
USA Ordnance Board	(1)
USA Quartermaster Board	(2)
USA QM Research and Engineering Command	(1)
USA QM Field Evaluation Agency	(2)
USA Signal Board	(1)
Chief of Transportation, DA	(6)
USA Transportation Combat Development Group	(1)
USA Transportation Board	(2)
USA Transportation Materiel Command	(20)
USA Transportation Training Command	(1)
USA Transportation School	(3)
USA Transportation Research Command	(44)
USATRECOM Liaison Officer, USA Engineer Waterways Experiment Station	(1)
USATRECOM Liaison Office, Wright-Patterson AFB	(1)
USATRECOM Liaison Officer, USA R&D Liaison Group (9851 DU)	(1)
TC Liaison Officer, USAERDL	(1)
USATRECOM Liaison Officer, Detroit Arsenal	(1)
USA Transportation Terminal Command, Atlantic	(1)

DISTRIBUTION (Continued)

USA Transportation Terminal Command, Pacific	(3)
USA TC Liaison Officer, Airborne and Electronics Board	(1)
USA Europe (Rear)/Communications Zone	(2)
Hq USATDS	(1)
US Army, Pacific	(1)
US Army, Alaska	(3)
Eighth US Army	(2)
US Army Transportation Agency, Japan	(1)
US Army, Ryukyu Islands/ IX Corps	(1)
US Army, Hawaii	(3)
US Army, Caribbean	(2)
Allied Land Forces Southeastern Europe	(2)
Air Research & Development Command	(1)
APGC (PGTRI), Eglin AFB	(1)
WADD(WWAD-Library)	(1)
Air University Library	(1)
Hq USAF (AFDFD)	(1)
Air Force Systems Command	(3)
Chief of Naval Research	(1)
Bureau of Naval Weapons	(7)
Asst. Chief for Research & Development (OW), Navy	(1)
US Naval Postgraduate School	(1)
David Taylor Model Basin	(1)
Hq, US Marine Corps	(1)
Marine Corps Schools	(3)
MC Liaison Officer, USA Transportation School	(1)
US Coast Guard	(1)
National Aviation Facilities Experimental Center	(10)
NASA, Washington, D.C.	(6)
George C. Marshall Space Flight Center, NASA	(4)
Langley Research Center, NASA	(3)
Ames Research Center, NASA	(1)
Lewis Research Center, NASA	(1)
Library of Congress	(2)
US Army Standardization Group, U.K.	(1)
US Army Standardization Group, Canada	(1)
Canadian Army Liaison Officer, USA Transportation School	(3)
British Joint Services Mission (Army Staff)	(3)
Armed Services Technical Information Agency	(10)
Institute of Aeronautical Sciences	(1)
Human Resources Research Office	(1)
Cornell Aeronautical Laboratory, Inc.	(12)

<p>AD- Cornell Aeronautical Laboratory, Inc., Buffalo, New York</p>	<p>UNCLASSIFIED</p> <p>1. VTOL Aircraft</p> <p>2. Contract DA-44-177-TC-699</p>	<p>THEORETICAL INVESTIGATION OF THE FLUTTER CHARACTERISTICS OF A JET-FLAP ROTOR SYSTEM IN HOVERING FLIGHT - Richard P. White Jr. and Peter Crimi.</p> <p>Report TCREC 61-142, November, 1961, pp. - (Contract DA 44-177-TC-699) USATRECOM TASK 9R38-13-014-03, Unclassified Report</p> <p>The results of a theoretical investigation conducted to determine the flutter characteristics of a jet-flap rotor system in hovering flight are presented. The rotor system analyzed was an underslung teetering rotor with flapping hinges. The amount the rotor was underslung and the offset of the flapping hinge were both varied in the analysis. The rotor also had a jet-flap over the outer 30% of blade radius that was used in place of cyclic and collective pitch control as well as for propulsion. The investigation determined the effect of changes in the elastic axis and center-of-gravity positions, the blowing coefficient, the nonrotating bending-to-torsion frequency ratio, and the frequency of the control flap on the flutter characteristics of the rotor system.</p>
---	---	--

<p>AD- Cornell Aeronautical Laboratory, Inc., Buffalo, New York</p>	<p>UNCLASSIFIED</p> <p>1. VTOL Aircraft</p> <p>2. Contract DA-44-177-TC-699</p>	<p>THEORETICAL INVESTIGATION OF THE FLUTTER CHARACTERISTICS OF A JET-FLAP ROTOR SYSTEM IN HOVERING FLIGHT - Richard P. White Jr. and Peter Crimi.</p> <p>Report TCREC 61-142, November, 1961, pp. - (Contract DA 44-177-TC-699) USATRECOM TASK 9R38-13-014-03, Unclassified Report</p> <p>The results of a theoretical investigation conducted to determine the flutter characteristics of a jet-flap rotor system in hovering flight are presented. The rotor system analyzed was an underslung teetering rotor with flapping hinges. The amount the rotor was underslung and the offset of the flapping hinge were both varied in the analysis. The rotor also had a jet-flap over the outer 30% of blade radius that was used in place of cyclic and collective pitch control as well as for propulsion. The investigation determined the effect of changes in the elastic axis and center-of-gravity positions, the blowing coefficient, the nonrotating bending-to-torsion frequency ratio, and the frequency of the control flap on the flutter characteristics of the rotor system.</p>
---	---	--

<p>AD- Cornell Aeronautical Laboratory, Inc., Buffalo, New York</p>	<p>UNCLASSIFIED</p> <p>1. VTOL Aircraft</p> <p>2. Contract DA-44-177-TC-699</p>	<p>THEORETICAL INVESTIGATION OF THE FLUTTER CHARACTERISTICS OF A JET-FLAP ROTOR SYSTEM IN HOVERING FLIGHT - Richard P. White Jr. and Peter Crimi.</p> <p>Report TCREC 61-142, November, 1961, pp. - (Contract DA 44-177-TC-699) USATRECOM TASK 9R38-13-014-03, Unclassified Report</p> <p>The results of a theoretical investigation conducted to determine the flutter characteristics of a jet-flap rotor system in hovering flight are presented. The rotor system analyzed was an underslung teetering rotor with flapping hinges. The amount the rotor was underslung and the offset of the flapping hinge were both varied in the analysis. The rotor also had a jet-flap over the outer 30% of blade radius that was used in place of cyclic and collective pitch control as well as for propulsion. The investigation determined the effect of changes in the elastic axis and center-of-gravity positions, the blowing coefficient, the nonrotating bending-to-torsion frequency ratio, and the frequency of the control flap on the flutter characteristics of the rotor system.</p>
---	---	--

<p>AD- Cornell Aeronautical Laboratory, Inc., Buffalo, New York</p>	<p>UNCLASSIFIED</p> <p>1. VTOL Aircraft</p> <p>2. Contract DA-44-177-TC-699</p>	<p>THEORETICAL INVESTIGATION OF THE FLUTTER CHARACTERISTICS OF A JET-FLAP ROTOR SYSTEM IN HOVERING FLIGHT - Richard P. White Jr. and Peter Crimi.</p> <p>Report TCREC 61-142, November, 1961, pp. - (Contract DA 44-177-TC-699) USATRECOM TASK 9R38-13-014-03, Unclassified Report</p> <p>The results of a theoretical investigation conducted to determine the flutter characteristics of a jet-flap rotor system in hovering flight are presented. The rotor system analyzed was an underslung teetering rotor with flapping hinges. The amount the rotor was underslung and the offset of the flapping hinge were both varied in the analysis. The rotor also had a jet-flap over the outer 30% of blade radius that was used in place of cyclic and collective pitch control as well as for propulsion. The investigation determined the effect of changes in the elastic axis and center-of-gravity positions, the blowing coefficient, the nonrotating bending-to-torsion frequency ratio, and the frequency of the control flap on the flutter characteristics of the rotor system.</p>
---	---	--

<p>AD-</p> <p>Cornell Aeronautical Laboratory, Inc., Buffalo, New York</p> <p>THEORETICAL INVESTIGATION OF THE FLUTTER CHARACTERISTICS OF A JET-FLAP ROTOR SYSTEM IN HOVERING FLIGHT -</p> <p>Richard P. White Jr. and Peter Crimi.</p> <p>Report TCREC 61-142, November, 1961, pp. - (Contract DA 44-177-TC-699) USATRECOM TASK 9R38-13-014-03, Unclassified Report.</p> <p>The results of a theoretical investigation conducted to determine the flutter characteristics of a jet-flap rotor system in hovering flight are presented. The rotor system analyzed was an underslung teetering rotor with flapping hinges. The amount the rotor was underslung and the offset of the flapping hinge were both varied in the analysis. The rotor also had a jet-flap over the outer 30% of blade radius that was used in place of cyclic and collective pitch control, as well as for propulsion. The investigation determined the effect of changes in the elastic axis and center-of-gravity positions, the blowing coefficient, the nonrotating bending-to-torsion frequency ratio, and the frequency of the control flap on the flutter characteristics of the rotor system.</p>	<p>UNCLASSIFIED</p> <p>1. VTOL Aircraft</p> <p>2. Contract DA-44-177-TC-699</p>
--	---

<p>AD-</p> <p>Cornell Aeronautical Laboratory, Inc., Buffalo, New York</p> <p>THEORETICAL INVESTIGATION OF THE FLUTTER CHARACTERISTICS OF A JET-FLAP ROTOR SYSTEM IN HOVERING FLIGHT -</p> <p>Richard P. White Jr. and Peter Crimi.</p> <p>Report TCREC 61-142, November, 1961, pp. - (Contract DA 44-177-TC-699) USATRECOM TASK 9R38-13-014-03, Unclassified Report.</p> <p>The results of a theoretical investigation conducted to determine the flutter characteristics of a jet-flap rotor system in hovering flight are presented. The rotor system analyzed was an underslung teetering rotor with flapping hinges. The amount the rotor was underslung and the offset of the flapping hinge were both varied in the analysis. The rotor also had a jet-flap over the outer 30% of blade radius that was used in place of cyclic and collective pitch control, as well as for propulsion. The investigation determined the effect of changes in the elastic axis and center-of-gravity positions, the blowing coefficient, the nonrotating bending-to-torsion frequency ratio, and the frequency of the control flap on the flutter characteristics of the rotor system.</p>	<p>UNCLASSIFIED</p> <p>1. VTOL Aircraft</p> <p>2. Contract DA-44-177-TC-699</p>
--	---

<p>AD-</p> <p>Cornell Aeronautical Laboratory, Inc., Buffalo, New York</p> <p>THEORETICAL INVESTIGATION OF THE FLUTTER CHARACTERISTICS OF A JET-FLAP ROTOR SYSTEM IN HOVERING FLIGHT -</p> <p>Richard P. White Jr. and Peter Crimi.</p> <p>Report TCREC 61-142, November, 1961, pp. - (Contract DA 44-177-TC-699) USATRECOM TASK 9R38-13-014-03, Unclassified Report.</p> <p>The results of a theoretical investigation conducted to determine the flutter characteristics of a jet-flap rotor system in hovering flight are presented. The rotor system analyzed was an underslung teetering rotor with flapping hinges. The amount the rotor was underslung and the offset of the flapping hinge were both varied in the analysis. The rotor also had a jet-flap over the outer 30% of blade radius that was used in place of cyclic and collective pitch control, as well as for propulsion. The investigation determined the effect of changes in the elastic axis and center-of-gravity positions, the blowing coefficient, the nonrotating bending-to-torsion frequency ratio, and the frequency of the control flap on the flutter characteristics of the rotor system.</p>	<p>UNCLASSIFIED</p> <p>1. VTOL Aircraft</p> <p>2. Contract DA-44-177-TC-699</p>
--	---

<p>AD-</p> <p>Cornell Aeronautical Laboratory, Inc., Buffalo, New York</p> <p>THEORETICAL INVESTIGATION OF THE FLUTTER CHARACTERISTICS OF A JET-FLAP ROTOR SYSTEM IN HOVERING FLIGHT -</p> <p>Richard P. White Jr. and Peter Crimi.</p> <p>Report TCREC 61-142, November, 1961, pp. - (Contract DA 44-177-TC-699) USATRECOM TASK 9R38-13-014-03, Unclassified Report.</p> <p>The results of a theoretical investigation conducted to determine the flutter characteristics of a jet-flap rotor system in hovering flight are presented. The rotor system analyzed was an underslung teetering rotor with flapping hinges. The amount the rotor was underslung and the offset of the flapping hinge were both varied in the analysis. The rotor also had a jet-flap over the outer 30% of blade radius that was used in place of cyclic and collective pitch control, as well as for propulsion. The investigation determined the effect of changes in the elastic axis and center-of-gravity positions, the blowing coefficient, the nonrotating bending-to-torsion frequency ratio, and the frequency of the control flap on the flutter characteristics of the rotor system.</p>	<p>UNCLASSIFIED</p> <p>1. VTOL Aircraft</p> <p>2. Contract DA-44-177-TC-699</p>
--	---

UNCLASSIFIED

UNCLASSIFIED